This project is part of the PRIMA Programme supported by the European Union

RESERVOIR

Sustainable groundwater RESources managEment by integrating eaRth observation deriVed monitoring and flOw modelIng Results

PRIMA

GA no. 1924

DELIVERABLE D5.1

Groundwater Flow Model for the Coastal Aquifer of Comacchio (Italy)

Author(s):	DEU: Alper Elçi, M. Berker Bayırtepe, Elif Aysu Batkan UNIPV: Claudia Meisina, Laura Pedretti CER: Tommaso Letterio
Responsible Partner:	DEU
Version:	Final
Date:	31 March 2023
Distribution Level (CO, PU)	PU

Acknowledgement

This project has received funding from the Partnership for Research and Innovation in the Mediterranean Area under the European Union's Horizon 2020 research and innovation programme under grant agreement No 1924.

Statement of Originality

This document contains original unpublished work except where clearly indicated otherwise. Acknowledgement of previously published material and of the work of others has been made through appropriate citation, quotation, or both.

Disclaimer

This publication reflects the authors' views. The consortium is not responsible for any use that may be made of the information it contains. The information contained in this document and any other information linked therein is confidential, privileged and it remains the property of its respective owner(s). As such, and under the conditions settled in the RESERVOIR Grant Agreement and the RESERVOIR Consortium Agreement, it is disclosed for the information of the intended recipients within the RESERVOIR Consortium and the European Commission / PRIMA according to its "Dissemination Level"* and may not be used, published or redistributed without the prior written consent of its owner(s).

* PU = Public; CO = Confidential, only for members of the consortium EU-R/R-UE = Classified, as referred to in Commission Decision 2001/844/EC.

DOCUMENT REVISION HISTORY

Date	Version	Editor(s)	Comments	Status
27.03.2023	0.1	Alper Elçi (DEU), Elif Aysu Batkan (DEU), Berker Bayırtepe (DEU)	Submitted for review by co-authors and project board	Draft
28.03.2023	0.2	Tommaso Letterio (CER)		Draft
28.03.2023	0.2	Roberto Tomas (UA)		Draft
28.03.2023	0.2	Claudia Meisina (UNIPD)		Draft
30.03.2023	0.2	Ali Hakan Ören (DEU)		Draft
31.03.2023	1.0	Alper Elçi (DEU), Berker Bayırtepe (DEU)		Final

LIST OF PARTNERS

Participant	Name	Country
UNIPV	Università degli Studi di Pavia	Italy
UNIPD	Università di Padova	Italy
IGME	Instituto Geológico y Minero de España	Spain
UA	Universidad de Alicante	Spain
DEU	Dokuz Eylül University	Turkey
UJ	The University of Jordan	Jordan
CER	Consorzio di Bonifica di secondo grado per il Canale Emiliano Romagnolo	Italy
RSCN-AWR	Royal Society for the Conservation of Nature - Azraq Wetland Reserve	Jordan

GLOSSARY

Acronym	Description
AOI	Area of Interest
C	Solute Concentration
CER	Consorzio di Bonifica di secondo grado per il Canale Emiliano Romagnolo

Acronym	Description
DEM	Digital Elevation Model
EC	Electrical Conductivity
EO	Earth Observation
GUI	Graphical User Interface
k	Permeability
MAE	Mean Absolute Error
P	Pressure
RMSE	Root Mean Squared Error
WP	Work Package

CONTENTS

LIST OF FIGURES AND TABLES

1. INTRODUCTION

1.1 Goal and Purpose of this Document

The RESERVOIR project aims to provide new products and services for a sustainable groundwater management model to be developed and tested in four water-stressed Mediterranean pilot sites and then be applicable in other regions via an interdisciplinary approach.

The specific Project Objectives (PO) are the following:

- PO1. Develop an innovative methodology for the hydrogeological characterization of large-scale aquifer systems using low-cost and non-intrusive data such as satellite-based Earth Observation (EO) techniques.
- PO2. Integrate advanced EO techniques into numerical groundwater flow and geomechanical models to improve the knowledge about the current capacity to store water and the future response of aquifer systems to natural and human-induced stresses.
- PO3. Enhance the knowledge about the impacts of agricultural and tourism activities on the water resources by quantifying the ground deformation during the monitored periods.
- PO4. Engage water management authorities and provide models for optimal management of the aquifer systems. We will engage 4 water authorities in 4 different countries through a series of face-to-face workshops (each participant will organize at least 1 workshop in the first 4 months of the project). The water authorities will be involved in the conceptualization and design of guidelines for Groundwater Resource Management (GRM). Best practices of water management for agricultural and tourism purposes will be developed taking advantage of the knowledge and methodologies from the outputs of PO1, PO2, and PO3.
- PO5. Dissemination and exchange of the generated knowledge among the experts and the managers in charge of land and groundwater management in the pilot sites to strengthen the aquifer resilience.

The main objective of WP5 is to develop groundwater flow models for all pilot sites. The models are calibrated against time series of historical hydraulic head measurements and the calibrated models are subsequently used to simulate groundwater flow for the analyzed period of EO data, i.e. processed A-DInSAR observation period. Through the integration of EO observations into these numerical groundwater flow models, the current capacity to store water and the future response of the aquifer to climate and global change-related stresses are simulated.

WP5 is subdivided into five tasks, corresponding to the groundwater flow models of each pilot site and an additional task (T5.5) that involves the implementation of the integration of D-InSAR with the flow models:

- T5.1 – Development, calibration, and application of the variable-density groundwater flow model for the coastal aquifer of Comacchio (Italy)
- T5.2 – Development, calibration, and application of the groundwater flow model for the Alto Guadalentín aquifer (Spain)
- T5.3 – Development, calibration, and application of the groundwater flow model for the alluvial aquifer of Gediz River Basin (Turkiye)

- T5.4 – Development, calibration, and application of the groundwater flow model for the Azraq Wetland Reserve (Jordan)
- T5.5 – Simulation results for the EO data-optimized GW flow models

In this deliverable, a detailed technical report of Task 5.1, the variable-density groundwater flow model for the Italy pilot site, the Goro-Gorino part of the coastal aquifer of Comacchio is presented. A three-dimensional, variably-saturated transient groundwater flow and transport model is developed for the coastal aquifer using Modelmuse version 5.1.1 (Winston, 2022), which is a public-domain GUI of the finite-element flow and solute transport model SUTRA (Voss and Provost, 2012). SUTRA is capable of simulating saturated and unsaturated groundwater flow under seawater intrusion conditions that cause fluid density variations thereby affecting flow.

1.2 Modeling Objectives

The specific objectives of this modeling study and the intended uses include the following:

1) To develop a mathematical model that helps understanding the spatial-temporal distribution of brackish groundwater beneath the reclaimed land of the Goro and Gorino municipalities;
2) To analyze different processes such as seawater intrusion and land subsidence due to natural and anthropogenic factors;
3) To estimate water and solute fluxes to and from the canals, rivers, and the sea;
4) To quantify the impact of freshwater sources on the freshening of the groundwater.

1.3 General Description of Model Area

The coastal aquifer of Comacchio (Italy) is located in the coastal floodplain of the Po River in the Emilia Romagna region of the Province of Ferrara (Northern Italy) and covers an area of 1,055 km^2. The coastal floodplain is limited to the North by one of the Po River branches, the Po di Goro, and to the South by the brackish water marshes of the Comacchio Lagoons. It is a reclaimed area with topography ranging from 14 to -5.8 m a.s.l. A large portion is composed of lowland zones below the sea level. The main water courses within the pilot site are Po di Goro, Po di Volano and Reno River and a man-made network of ditches and channels more than 1,850 km long used to keep farmland dry and managed by the Reclamation Authorities.

The modelling study within the scope of the RESERVOIR project was performed for a smaller part of the Comacchio aquifer, which is referred to as the Bonello basin. This basin with an area of about 20 km^2 is a sub-basin of the larger hydrological basin of Burana-Po di Volano (2400 km^2) that included almost the entire district of Ferrara and small portion of the Manova district (Galbiati et al., 2006). The study area is heavily drained with a dense network of ditches and channels. Most of the area is below sea level. The boundaries of the area of interest (labelled as “land area”), and boundaries of the model domain are shown in Figure 1-1. The eastern boundary of the area of interest (AOI) is defined by the Po di Goro River. The southern boundary is delineated by the coastline of the Sacca di Goro lagoon, while the Canale di Bianco delimits the area in the west. The study area is referred to as the “Goro-Gorino site” from here on.

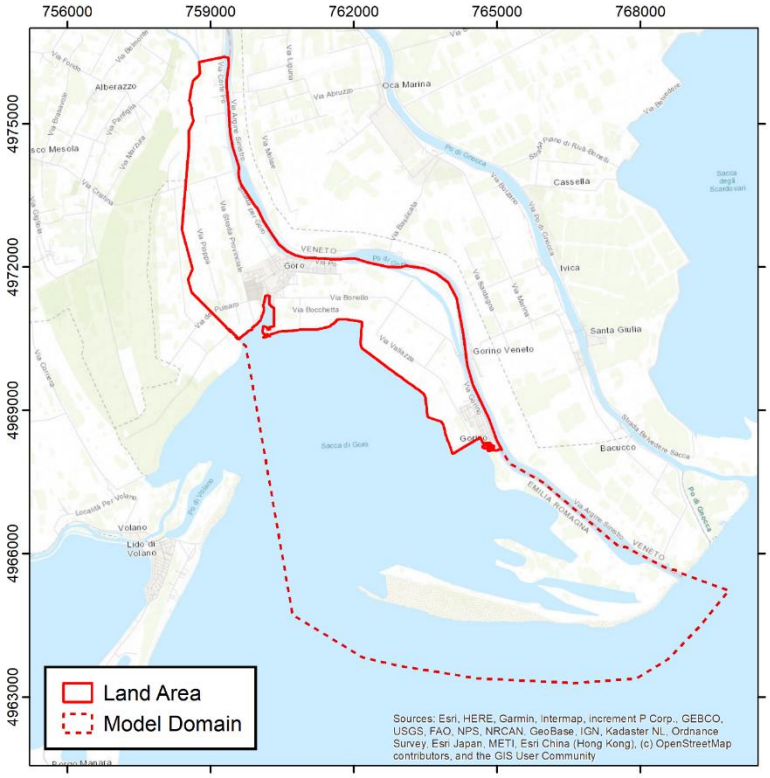

Figure 1-1. The geographic location of the Goro-Gorino pilot site.

1.3.1 Climatic Setting

The climate of the Goro-Gorino site is temperate and characterized by cold winters and warm summers with modest diurnal (10-12 °C) and annual temperature ranges (20-25 °C). At the nearest meteorological station, Giralda, the average annual rainfall is recorded at 630 mm over the period 2012-2020, which is evenly distributed throughout the year. As can be seen in Figure 1-2, there is a significant variability in rainfall patterns both across and within years. The within-year rainfall pattern varies between seasons, with the highest amount generally coinciding with the months from October to December. Across years, a sensible variation of the total amount of rain can be seen, with 2012 and 2013 the driest and the wettest years, respectively. The rainfall distribution follows the seasonality with higher amounts from October to March. The inter-annual variability of rainfall amount in spring (April-June) is very high and can affect the irrigation season. The seasonal yearly irrigation/rainfall regime affects the recharge of the shallow groundwater systems and, consequently, control at least in part the intrusion and encroachment of the seawater in the coastal aquifers and canals.

The evapotranspiration estimated with the Hargreaves equation (Hargreaves and Samani, 1985) shows lower variability across years and a stable seasonality can be identified where peak values occur from April to September (Figure 1-3). This period coincides with the irrigating season, where the difference between the potential evapotranspiration and the total precipitation is the highest. In Figure 1-4, the monthly average of precipitation and evapotranspiration is compared.

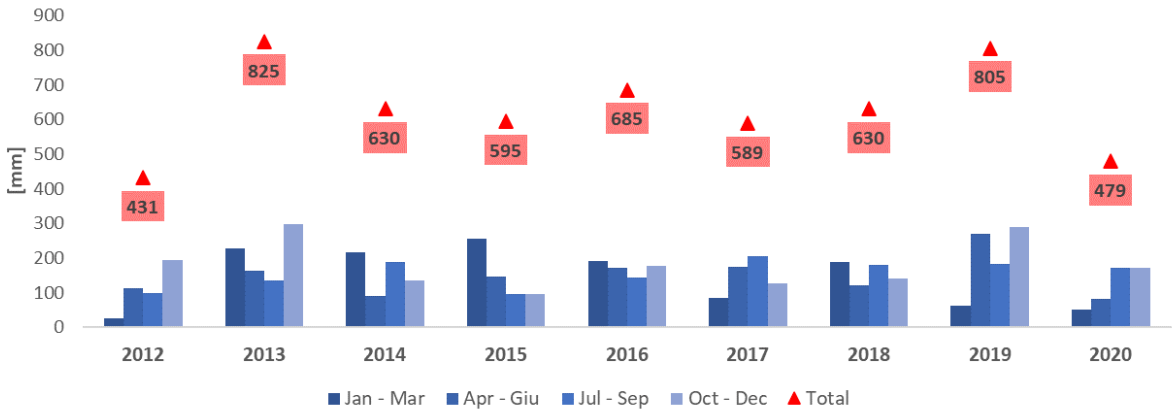

Figure 1-2. Temporal distributions of rainfall for the Goro-Gorino site.

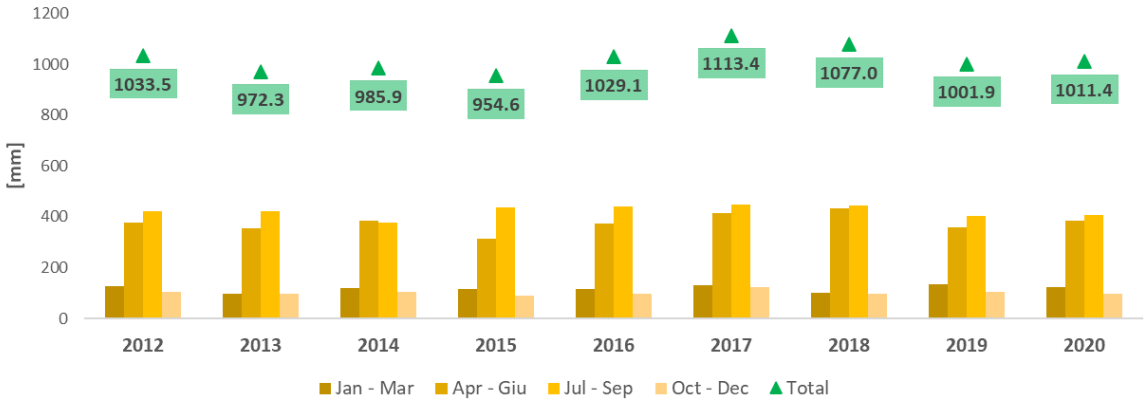

Figure 1-3. Temporal distributions of evapotranspiration for the Goro-Gorino site.

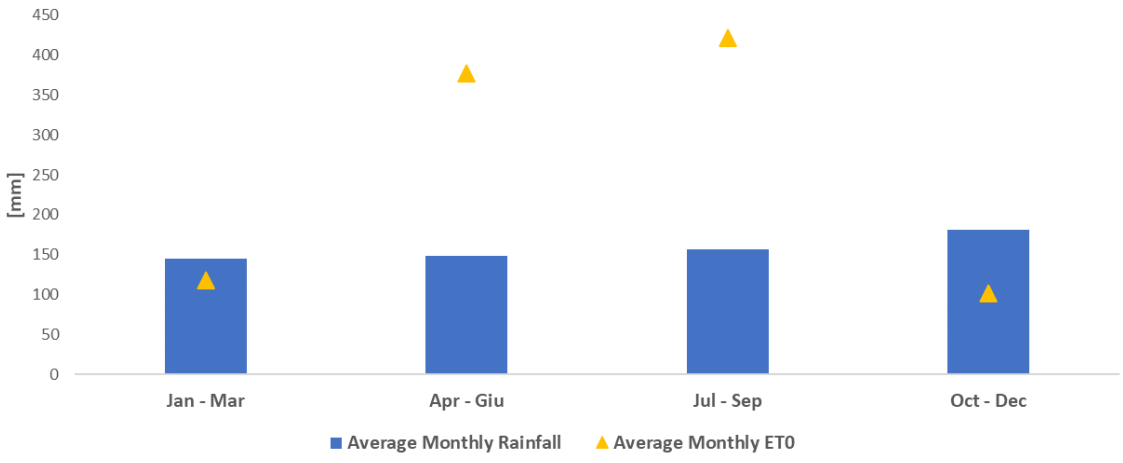

Figure 1-4. Comparison of monthly averages of rainfall and evapotranspiration.

1.3.2 Geological Setting

The study area is characterized by a complex aquifer geometry due to the depositional evolution of the Po Delta system. Natural subsidence and large sediment input supported a late Quaternary transgressive–regressive evolution in the Po Delta area (Stefani and Vincenzi, 2005). The area is located between the Apennines folding front and the south-dipping Venice monocline as shown in Figure 1-5, a structural framework characterized by active tectonic subsidence, which is enhanced by sediment compaction and anthropogenic factors (Bondesan et al., 1997).

Stefani and Vincenzi (2005) studied the depositional history of the Po Delta system and recognized that eustatic and climatic fluctuations dominated the depositional history of the area. Meanwhile, subsidence due to tectonic and sediment compaction had a significant contribution to the relative sea level increase, mainly during the "eustatically stable" highstand interval. The authors highlighted that spatial gradient of natural subsidence probably influenced the maximum transgression coastline configuration and the continental drainage network development, but not the geometry of the depositional sequence.

The sedimentary depositional sequence is characterized by shallow prograding sandy deltaic lobes and strand plains overlapped to transgressive bay and barrier deposits. From East to West, most of the sedimentary units consists of a wedge of permeable sandy sediments with intercalation of peat and silty layers. Littoral sands formed in the foreshore and in the adjacent beach, and sand dune systems. Coastline migration and different phases in the Po Delta progradation caused a series of coastal sand ridges (paleodunes) and paleo marsh lagoons (Simeoni and Corbau, 2009).

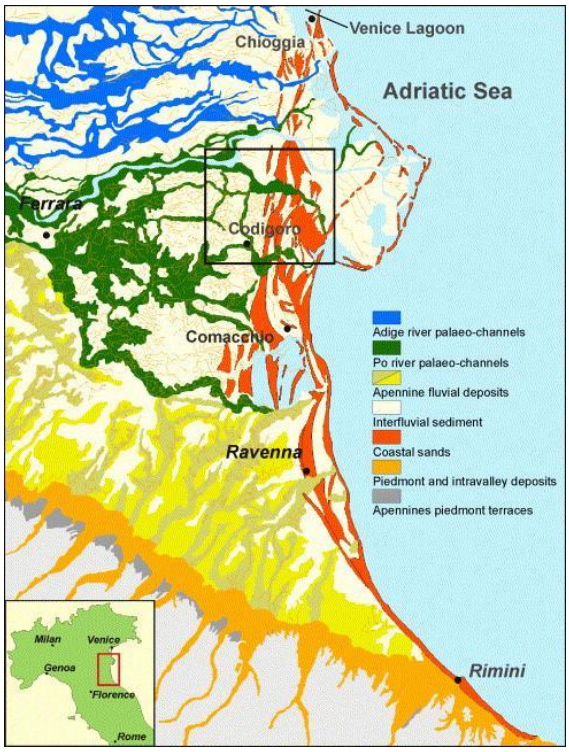

Figure 1-5. Geological setting of the coastal aquifer of Comacchio (Stefani and Vincenzi, 2005).

1.3.3 Land Use and Land Cover

Land use and land cover in the Goro-Gorino study site is composed of agricultural (54.0%), forest areas (10.29%), wetlands (14.32%) and water bodies (13.63%), and artificial surfaces (7.76%). The study site is characterized mostly by agricultural areas (14.53 km^2), that mainly consist of permanently irrigated lands. Around 85% of the irrigated land is intensively cultivated by maize and soybeans (Galbiati et al., 2006). The artificial surfaces correspond to the urban areas of the Goro-Gorino Municipality.

2. CONCEPTUAL MODEL

The following sections present the conceptualization of the Goro-Gorino site for the setup of the groundwater flow model based on previous studies, published information about the site, borehole logs, and geophysical survey results. Included are descriptions of the geologic aspects of the aquifer system, hydrologic boundaries, sources and sinks of groundwater, and information on hydraulic properties such as hydraulic conductivity and storage.

2.1 Aquifer System

The Goro-Gorino coastal aquifer is located in the southern part of the Po River Delta, with the land surface mostly below sea level (approximately -1.5 m a.s.l.). The area is characterized by a shallow depth to the water table. The groundwater fluxes are governed by the superficial drainage system consisting of a dense network of reclamation ditches (Figure 2-1). These ditches haves a multiple-use function in some parts of the network; during winter and rainfall the ditches act as drainage systems to prevent flooding, whereas during the summer they are used as irrigation channels for water transmission and distribution to the farmlands. The water height in the ditches is controlled by pumping stations and gates. The NE and S boundaries of the Goro-Gorino site are the Po di Goro River and the Sacca di Goro Lagoon (Adriatic Sea).

The aquifer system is defined by three stratigraphic units (from shallow to deep): (1) the shallow coastal aquifer formed by sandy littoral and delta deposits interbedded with silty-clay lenses (few meters thick), (2) marine deposits in the form of a silty clay layer, which acts as a saline aquitard (about 25 m thick, and (3) deeper alluvial deposits in the form of a sand layer. The model represents this aquifer system with seven model layers that have variable layer thicknesses. Information about layer thicknesses is given in section 3.1.

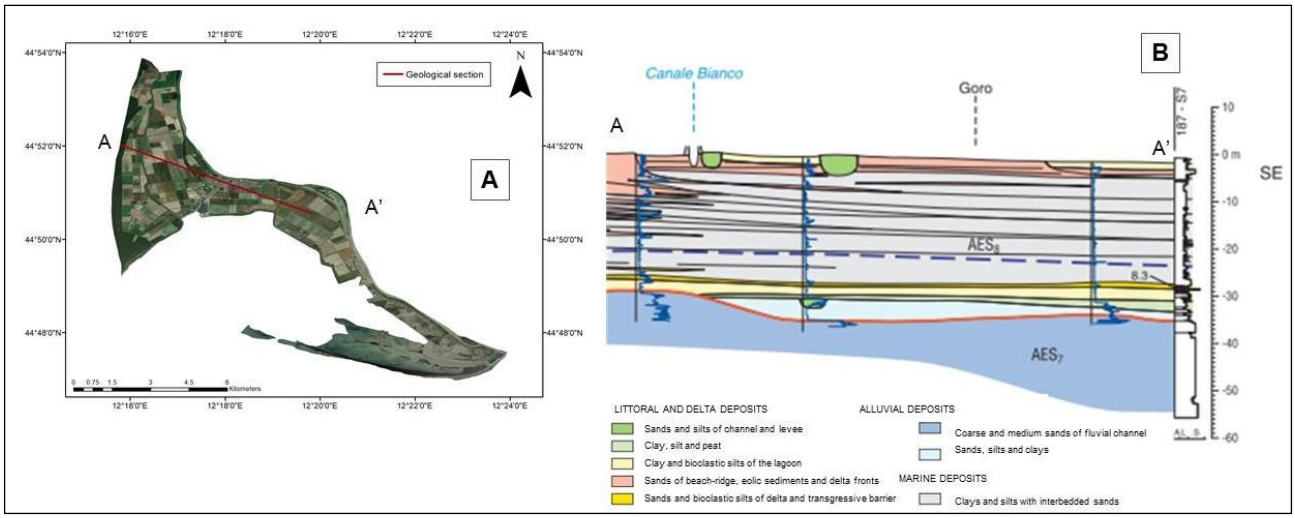

Figure 2-1. A representative geological cross-section at the Goro-Gorino site.

2.2 Sources and Sinks

The main inflows for the Goro-Gorino site are recharge via infiltrated precipitation, seasonal freshwater infiltration from irrigation ditches, influx from the Po di Goro River, and seawater intrusion from the Sacca di Goro lagoon. There is strong seawater intrusion especially in the summer season. Seasonal seepage to the main drainage ditches and evapotranspiration are the main outflow components. Overall, in this lowland area, which is under the influence of saline groundwater, fresh groundwater lenses are created by percolation of rainwater and/or leakage from ditches and canals. The freshening of groundwater allows plant growth and consequently supports both agriculture and natural vegetation.

2.2.1 Rivers and Canals

The northeast and south boundaries of the AOI are defined by the Po di Goro River and by the Sacca di Goro lagoon (part of the Adriatic Sea), respectively. It is known that a large quantity of water is entering the aquifer through these boundaries because of the strong hydraulic gradient between the catchment, having a land surface elevation ranging 1–2 m below the mean sea level, and the Po di Goro and Adriatic Sea, which have higher elevations (Galbiati et al., 2006). The main freshwater inputs are represented by i) Po di Volano River (about 3.5×10^8 m^3/yr), ii) a few canals with similar discharge ($2.0–5.5 \times 10^7$ m^3/yr each), called Giralda, Romanina, and Canal Bianco, that flow directly into the western part of the Sacca di Goro Lagoon, and iii) from the Po di Goro deltaic branch, which is artificially controlled through a dam in its eastern part.

2.2.2 Recharge

Due to the flat land surface, runoff can be assumed as negligible, therefore most of the rainfall can be considered as a recharge source for the Goro-Gorino aquifer. According to one of the previous studies for northern Italy (Kjaer, 2002), aquifer recharge in this area is in the order of 200 mm/year. As the aquifer is very shallow (0 to -3 m below sea level), almost 100% of the water percolating through the soil layer converts to direct groundwater recharge. Therefore, percolation below the root zone is assumed to reach the water table without a long delay.

2.2.3 Irrigation/Reclamation Ditches

In the study area, ditches are used to drain excess groundwater to keep the land dry. These ditches also serve as conduits for irrigation water. The ditches lay on the silty sand sediments and the depth of the channel bed is approximately 1.80 m below land surface. The width of the ditches is 2.50 m. The network of ditches is illustrated in Figure 2-2.

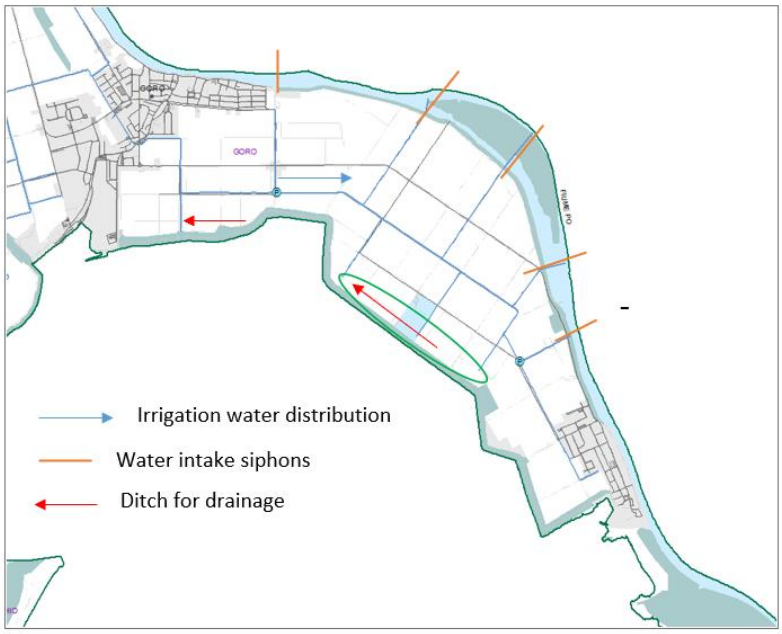

Figure 2-2. Network of ditches facilitating drainage of land and the distribution of irrigation water at Goro-Gorino site. Siphon river water intakes transfer water from the river to the irrigation system.

2.2.4 Marine Inflows

Also, the Goro-Gorino aquifer is partly connected to the sea. The marine inflows, varying according to the tidal dynamics, come from two mouths connecting the Sacca di Goro lagoon to the Northern Adriatic Sea. The area is characterized by large daily fluctuations of the water table due to the height of the tides, and seasonal fluctuations in the physicochemical parameters of the lagoon's water (temperatures: 2–33°C, salinity: 6–30 ppt, and pH: 7.0–8.8). The lagoon's bottom consists of silty-clay sediments, carried to the sea by rivers, but there are also sandy areas, particularly near the lagoon mouths and behind the spit and the barrier island (Corbau et al., 2016).

The coastal aquifer is influenced by autonomous salinization that is caused by influxes of hypersaline groundwater originating from the underlying silty clay aquitard (Giambastiani et al., 2013, Colombani et al., 2015). This aquitard is hydraulically connected to the Adriatic Sea and is referred to as the prodelta wedge.

2.3 Hydraulic Properties

A literature review is performed to collect information about hydrogeological parameters and physical properties hydraulic properties find the parameters for the hydrogeological modelling. The results are summarized in Table 2.7.

Table 2-1. Hydraulic parameters obtained from previous hydrogeological studies of the Goro-Gorino site.

Parameter	Literature
Hydraulic conductivity	The hydraulic conductivity of 1.0×10^{-4} m/s for the shallow unconfined aquifer and 3.0×10^{-4} m/s for the deep confined aquifer (Galbiati et al., 2006)
Aquifer vertical anisotropy	Isotropy (Galbiati et al., 2006)
Canal properties	Average depth: 0.8 m (Colombani et al., 2016)
Agricultural drain properties	Conductance: 1×10^{-4} m/s (Colombani et al., 2014)
Riverbed conductance	$1x10^{-6}$ m/s (Colombani et al., 2016)
Effective porosity	5.6×10^{-4} and 0.01 (Galbiati et al., 2006)
Specific yield	5.6×10^{-4} (Galbiati et al., 2006)
Specific storage	The storage properties of the aquifers were assumed constant for the entire area. The storage coefficient was fixed at 3.3×10^{-5} m^{-1} (Galbiati et al. 2006)

3. MODEL CONSTRUCTION

Groundwater flow under the influence of seawater intrusion in the Goro Gorino aquifer is simulated using the finite-element variable-density groundwater flow with solute transport model SUTRA 2.2. The model was constructed with Modelmuse 5.1.1 (Winston, 2022), an interface of SUTRA 2.2, and various other models developed and maintained by the U.S. Geological Survey, USGS.

SUTRA uses a Galerkin finite-element approach to solve the coupled equations of density-dependent flow and solute transport, under variably saturated or fully saturated groundwater flow conditions. In this study flow conditions are assumed to be fully saturated since the water table in the study area is considerably shallow, therefore the contribution to the aquifer from the water storage of the relatively thin vadose zone can be ignored. The governing equation that represents the fluid mass balance at every point in the variable-density groundwater in saturated porous media is:

$$\frac{\partial p}{\partial t}(\rho S_{op}) + \frac{\partial C}{\partial t}\left(\varepsilon \frac{\partial \rho}{\partial C}\right) = \frac{\partial(\varepsilon\rho)}{\partial t} \qquad \text{(Equation 1)}$$

where

p	is the fluid pressure (L);
C	solute concentration (T^{-1});
ρ	groundwater density (M/L^3);
ε	effective porosity (-)
S_{op}	is the specific pressure storativity of the porous medium (L^{-1});
t	time (T)

Groundwater flow resulting from fluid pressure and density variations is expressed in SUTRA by a general form of Darcy's Law:

$$v = -\frac{k}{\varepsilon\mu}(\nabla p - \rho g) \qquad \text{(Equation 2)}$$

where;

v	average fluid velocity (L/s);
k	solid matrix permeability (L^2);
μ	viscosity (M/(L·s));
∇p	divergence of fluid pressure;
g	gravitational acceleration (L/s^2)

Solute representing salinity in a coastal aquifer mass is transported through the aquifer by flow of groundwater. As the actual flow velocities of the groundwater may vary considerably in space, an average flow velocity is used, which is calculated from Darcy's Law (Equation 2). The advective-dispersion equation for a non-reactive, non-adsorbing solute is expressed as follows:

$$\frac{\partial(\varepsilon\rho C)}{\partial t} = -\nabla(\varepsilon\rho v C) + \nabla[\varepsilon\rho(D_m + \alpha v)\nabla C] + \varepsilon\rho\Gamma_w + Q_p C^* \qquad \text{(Equation 3)}$$

where;

D_m	molecular diffusion coefficient of solute in groundwater (L^2/s);
α	dispersivity tensor (L)
Γ_w	solute mass source in groundwater (M/M.s)
Q_p	groundwater source ($M/(L^3 \cdot s)$)
C^*	solute concentration of groundwater sources (M/M)

3.1 Spatial and Temporal Discretization

The three-dimensional model domain is discretized using an irregularly connected finite-element mesh that is extended vertically to the bottom of the domain. Horizontally, the mesh is generated with quadrilateral elements with maximum lateral lengths of 200 m. The mesh is refined with smaller elements with lateral lengths of 50 m along the coastline and around the irrigation ditches. The model domain covers a surface area of 15.77 km^2. The finite-element mesh for the model domain is presented in Figure 3-1. The three main stratigraphical units are further divided vertically into a total of 7 variably spaced layers of elements. Model layer 1 is divided into 2 layers, the silty-clay layer representing the aquitard is divided into three layers as it is relatively thicker. The deepest layer, model layer 3, is divided into 2 layers. Thicknesses of each model layer are given in Figure 3-2, where total thicknesses of model layers corresponding to the stratigraphic layers are shown. Furthermore, a cross-section of the model mesh is demonstrated in Figure 3-3. The resulting mesh contains 83167 elements and 96536 nodes. The projection used for geospatial data management in Modelmuse is WGS 1984 datum, Universe Transverse Mercator projection zone 32N (EPSG 32632). Numerical model spatial units are in meters.

The flow model is temporally discretized into a series of discrete time steps. In each time step, all hydrologic stresses are assumed to be constant, and any model output applies to the end of each time step. The model is discretized into 108 monthly time steps over the simulation period that begins in January 2013 and ends in December 2021. The constant time steps of the model are assigned using units of seconds, consequently resulting in $2.83824 \cdot 10^8$ seconds of simulation time. The runs of the transient model are transient in both pressure and concentrations.

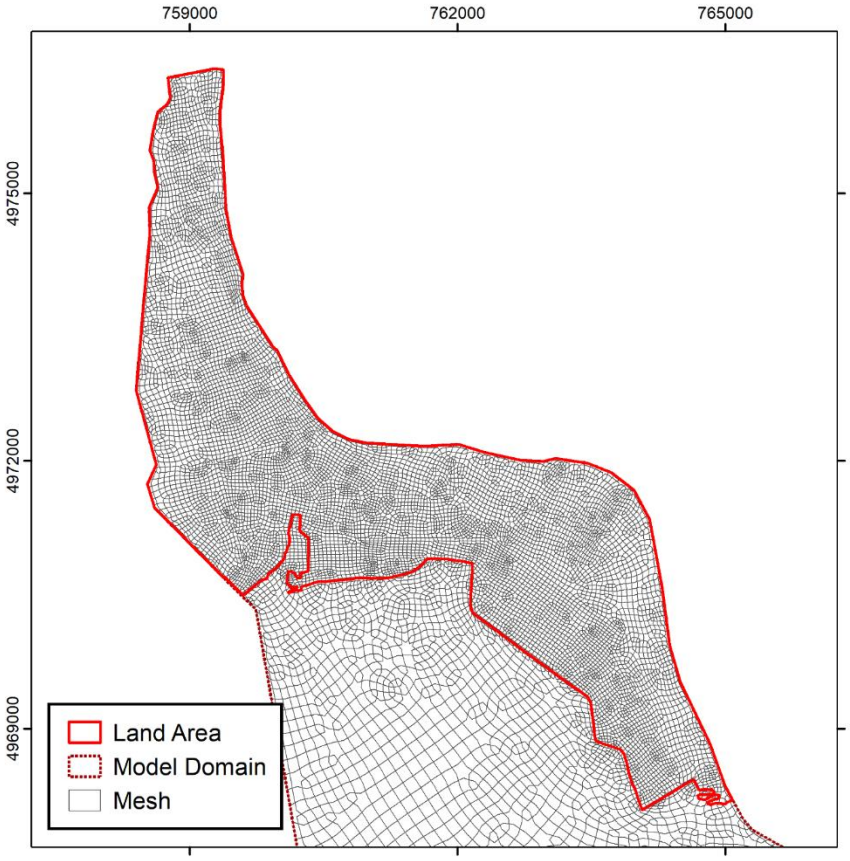

Figure 3-1. Numerical flow model mesh for the Goro-Gorino site with variable spatial resolution.

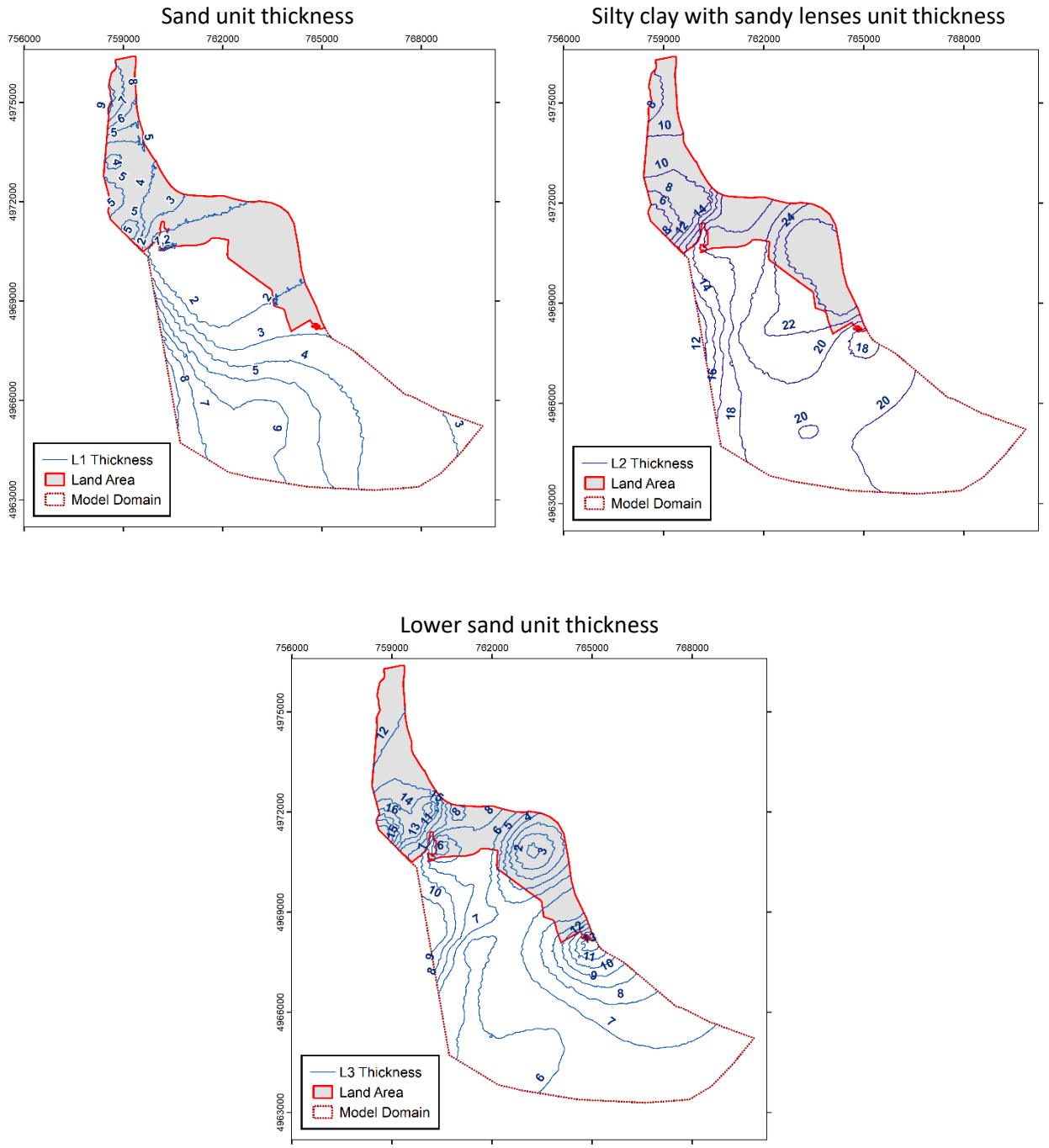

Figure 3-2. Thickness contour maps of each model layer.

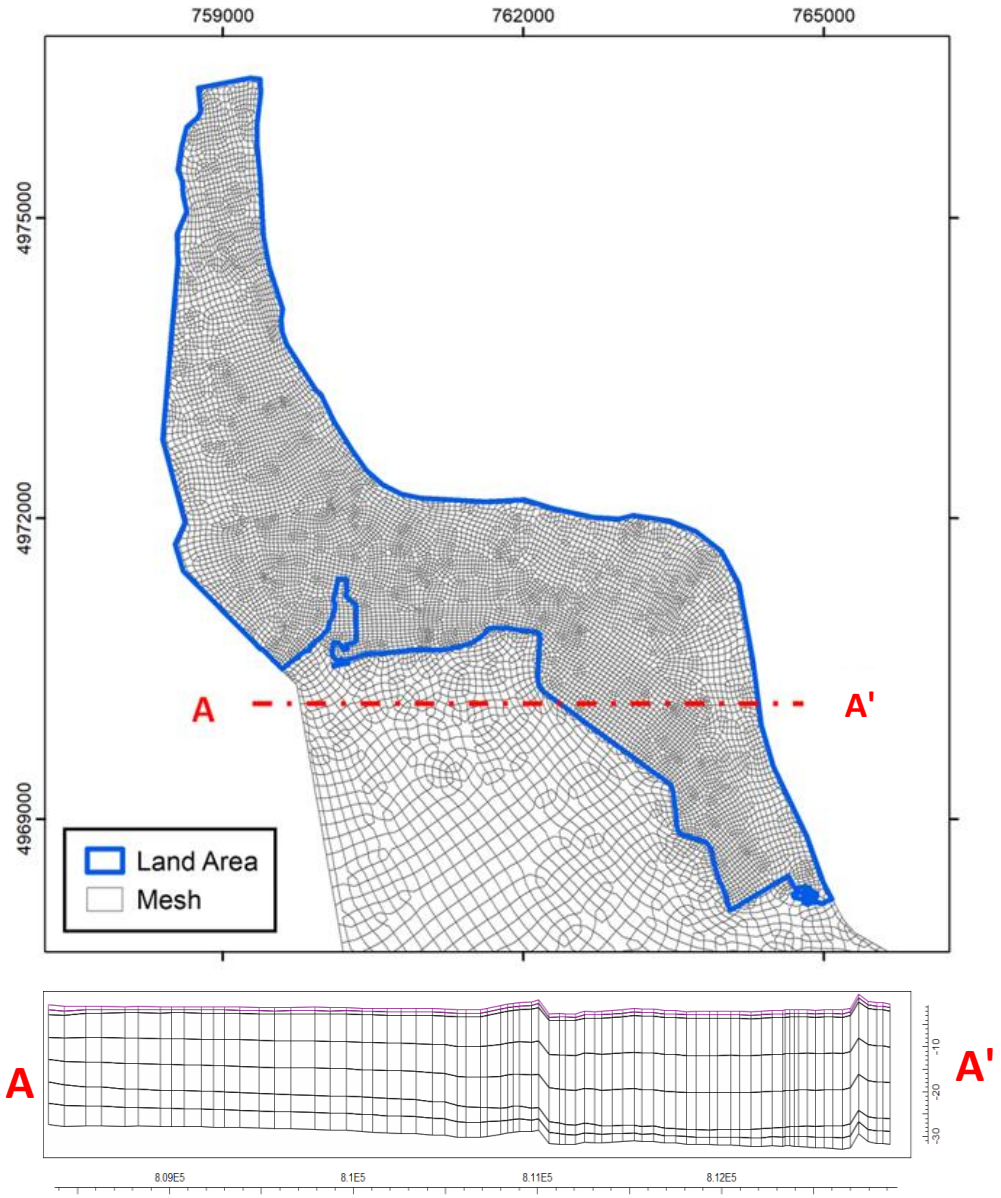

Figure 3-3. Cross-section of the model mesh for the Goro-Gorino coastal aquifer flow model.

3.2 Initial Conditions

The initial head distribution of the flow model is determined by running a warm-up simulation using temporally averaged groundwater recharge and water height in the ditches. In the warm-up model, associated salinity concentrations at the specified pressure boundary representing the river are obtained by taking the average of the time series. The initial concentration distribution is set at seawater concentration everywhere in the model domain. The warm-up model is run steady-state in pressure and transient in concentration. After 48 monthly time steps, steady-state solutions for pressure and solute concentration are reached, which are used as initial conditions in the transient model. Maps of the initial pressure and concentration distributions assigned to each model layer are shown in Figure 3-4 and Figure 3-5, respectively.

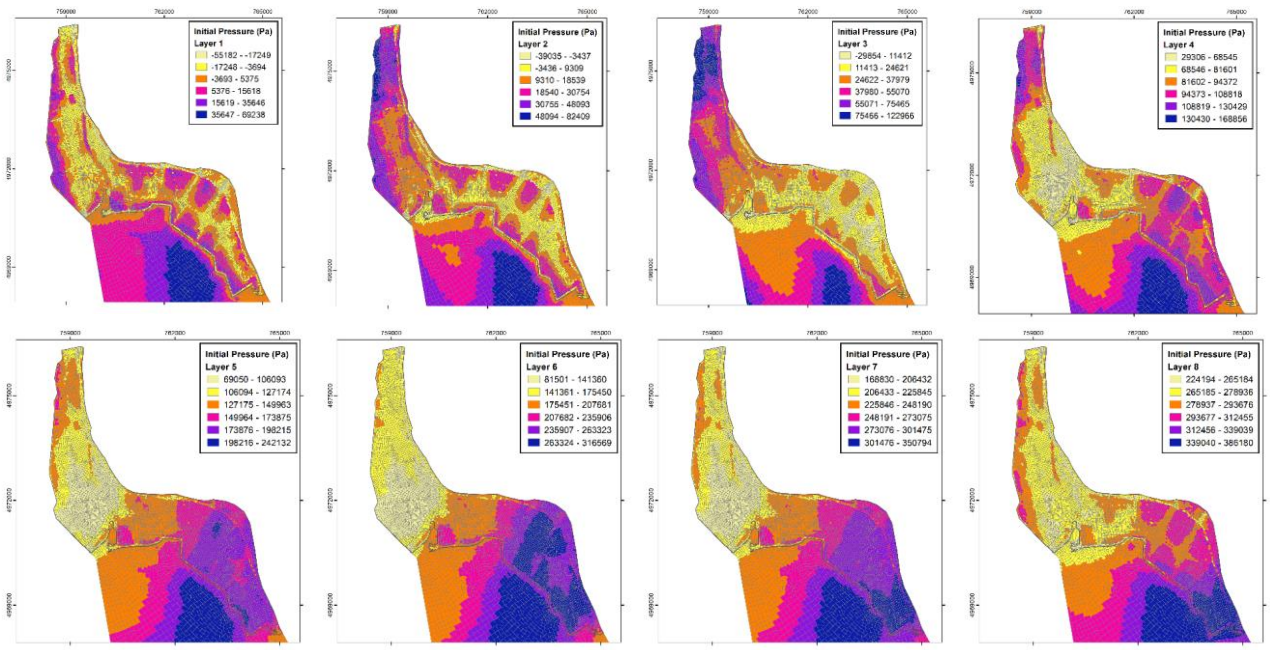

Figure 3-4. Initial conditions representing the groundwater pressure distributions in January 2013 were assigned to model layers 1 through 7.

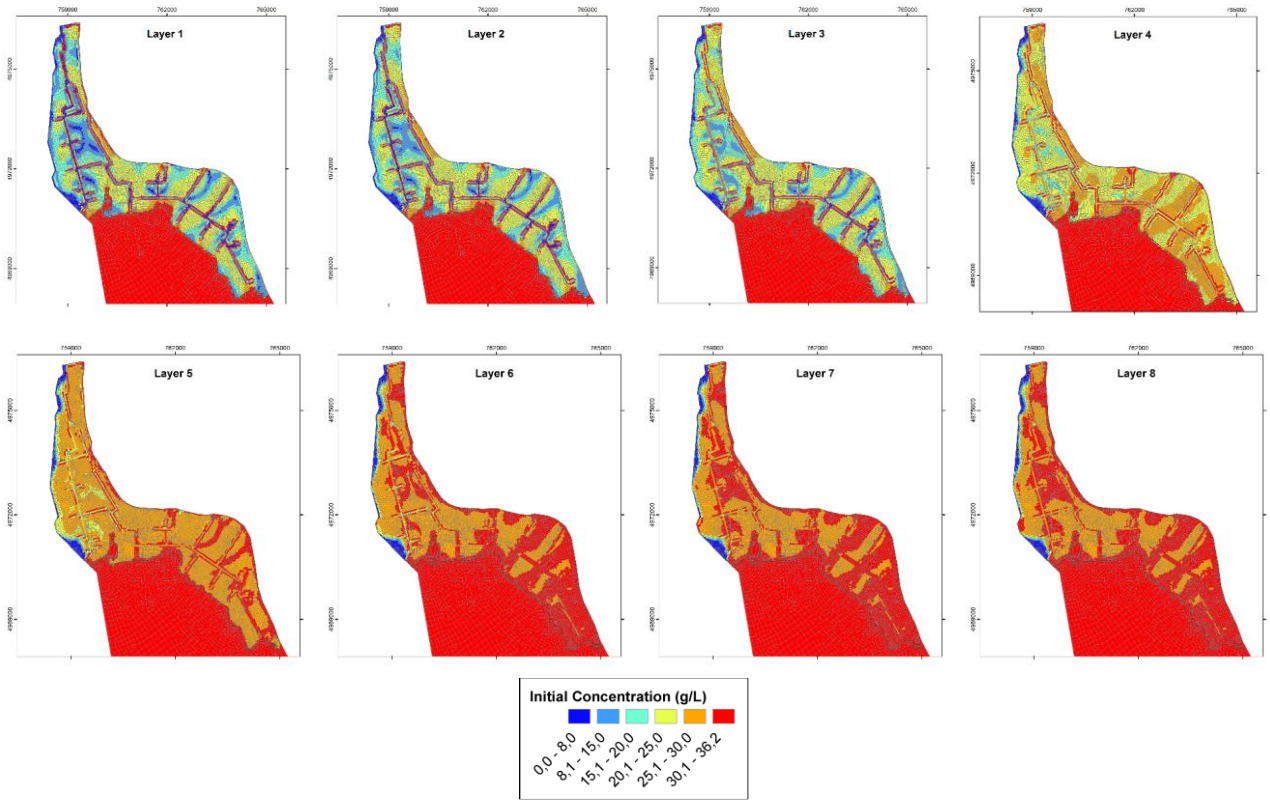

Figure 3-5. Initial conditions representing the solute concentration distribution in January 2013 assigned to model layers 1 through 7.

3.3 Boundary Conditions

3.3.1 External Boundaries: River, Canal and Others

Different boundary conditions are identified along the periphery of the model domain. External and internal boundary conditions that are assigned in the flow model are shown in Figure 3-6. All lateral boundaries are set as specified pressure (SP) boundaries by assuming hydrostatic pressure in all model layers. No flow is set to occur across the bottom of the model domain. In the west, the model domain is bounded by the canal 'Canale Bianco', which was specified a salinity of C_{canal} = 0.87 g/L. The eastern boundary is delineated by the Po di Goro river. Assigned solute concentrations along the river boundary are provided in Figure 3-7. Continuous measurements of water electrical conductivity (EC) were recorded at 5 siphons along the river that are installed at different locations along the river shoreline to regulate the flow and provide irrigation water to the ditches. The salinity monitoring data was provided by CER. Using this data the solute concentration time series shown in Figure 3-7 are obtained. Concentration values of the river water for segments between siphons are determined by linear interpolation. The range of concentration values specified in the model is C_{canal} = 0.22 – 6.42 g/L. The south model boundary represents the Sacca di Goro Lagoon (Adriatic Sea) and the north model boundary is part of an irrigation ditch. The short model boundary in the north coincides with a ditch, therefore this boundary is assigned properties of a ditch, which are explained in the next section.

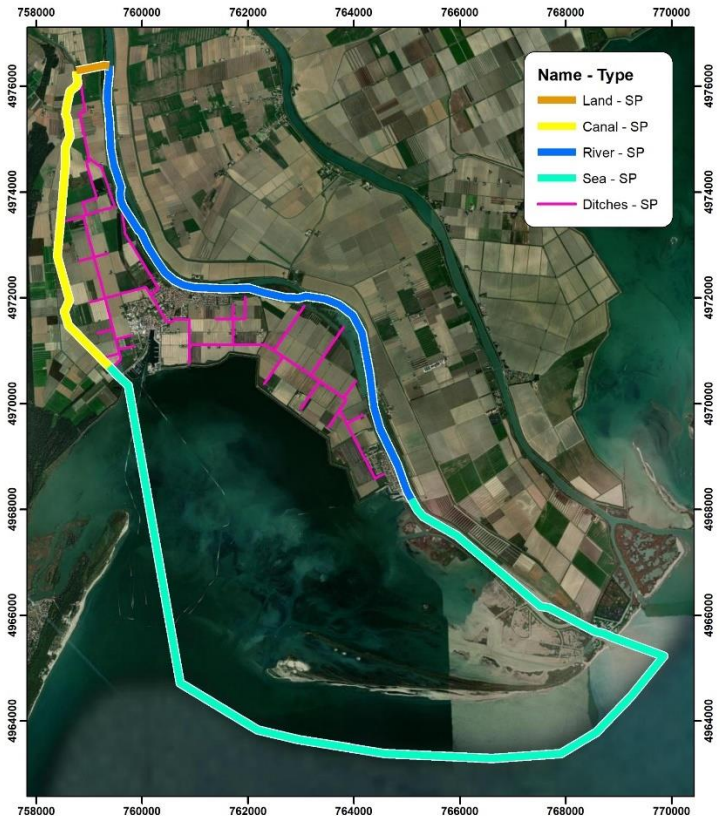

Figure 3-6. External boundary conditions assigned in the SUTRA model.

3.3.2 Internal Boundaries: Irrigation/Reclamation Ditches

The irrigation/reclamation ditches are assigned as internal specified pressure boundaries with associated solute concentrations. The top two nodes of model layer 1 are assigned boundary conditions. As the water height is seasonally variable, specific pressure is set as time-variable. Based on water management practices in the field, the water height in the ditches is maintained at a higher level during the irrigation season. The water depth is kept at approximately 0.8 m during the irrigation season, and 0.2 m during the winter months. It is assumed in the model that the two different water heights alternate every 6 months. The assigned time-variable water depths in the ditches are shown in Figure 3-8.

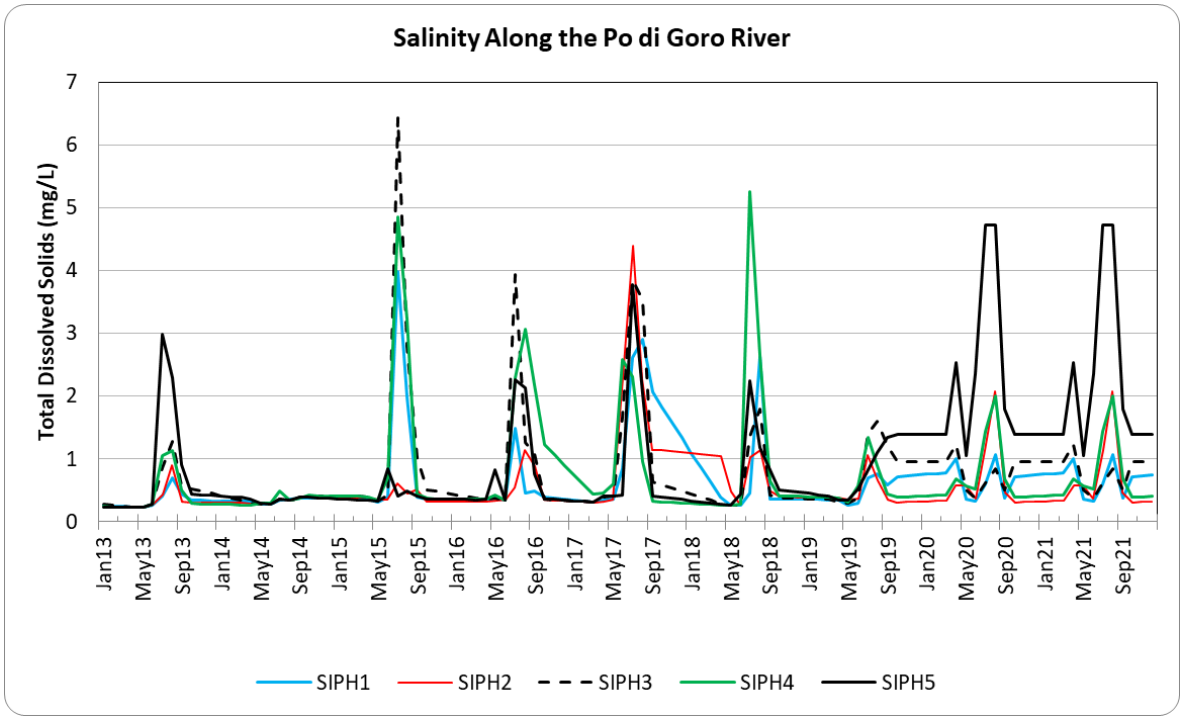

Figure 3-7. Salinity measurements at the five siphons along the Po id Goro River.

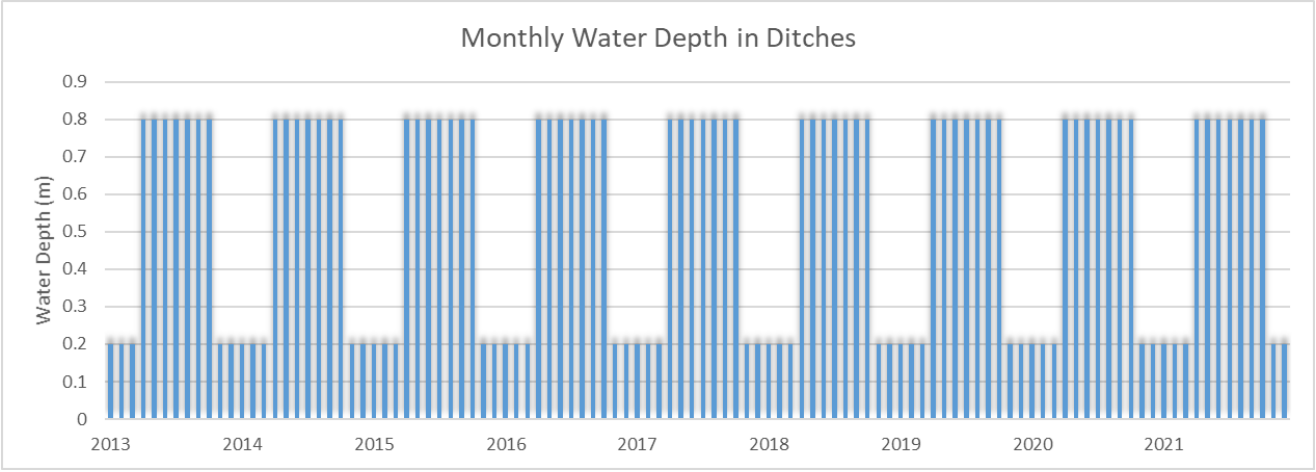

Figure 3-8. Seasonally changing water depths in the ditches.

3.3.3 Effective Precipitation

The effective precipitation rate is the net groundwater recharge that reaches the water table. It is calculated in this study as the difference between the rate of water infiltrating the soil and the evapotranspiration rate. IRRINET (Mannini et al., 2013), an expert system developed by CER for irrigation scheduling, is used to estimate infiltration rates, irrigation water demand, irrigation return flow and evapotranspiration. IRRINET is a water balance model that simulates the water dynamics in the soil layers. The effective precipitation rates resulting from IRRINET are applied to the uppermost layer of nodes as a time-variable fluid flux boundary. Monthly average rates of infiltration, evapotranspiration, and effective precipitation are presented in Table 3-1 and Figure 3-9. During the simulation period, effective precipitation is estimated to range between -5.2 and 4.8 mm/d with a mean of 0.301 mm/d indicating a net influx of freshwater to the aquifer. In terms of m3/month, this net influx corresponds to 0.1405 Mm^3/mo, which results in a cumulative freshwater source of 15.177 Mm^3 over the 9-year simulation period, and an average annual rate of 1.686 Mm^3/yr, and an average of 106.9 mm/yr normalized over the AOI. Time series of monthly net effective precipitation that were assigned in the model are presented in Figure 3-10.

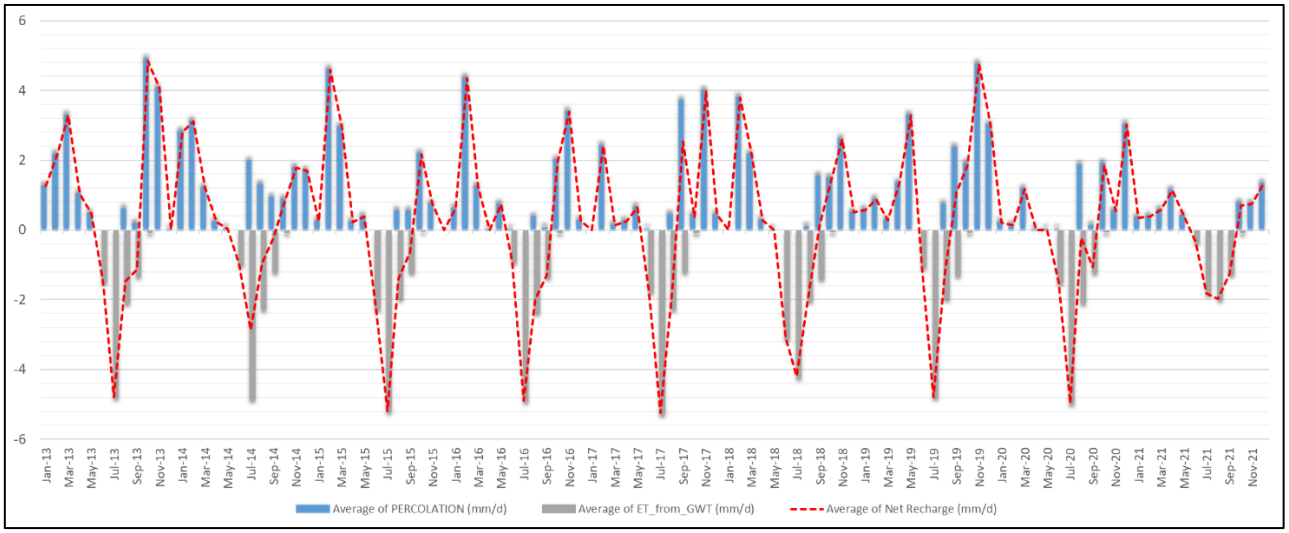

Figure 3-9. Monthly infiltration, evapotranspiration, and net recharge rates (effective precipitation) in mm/d assigned as model input.

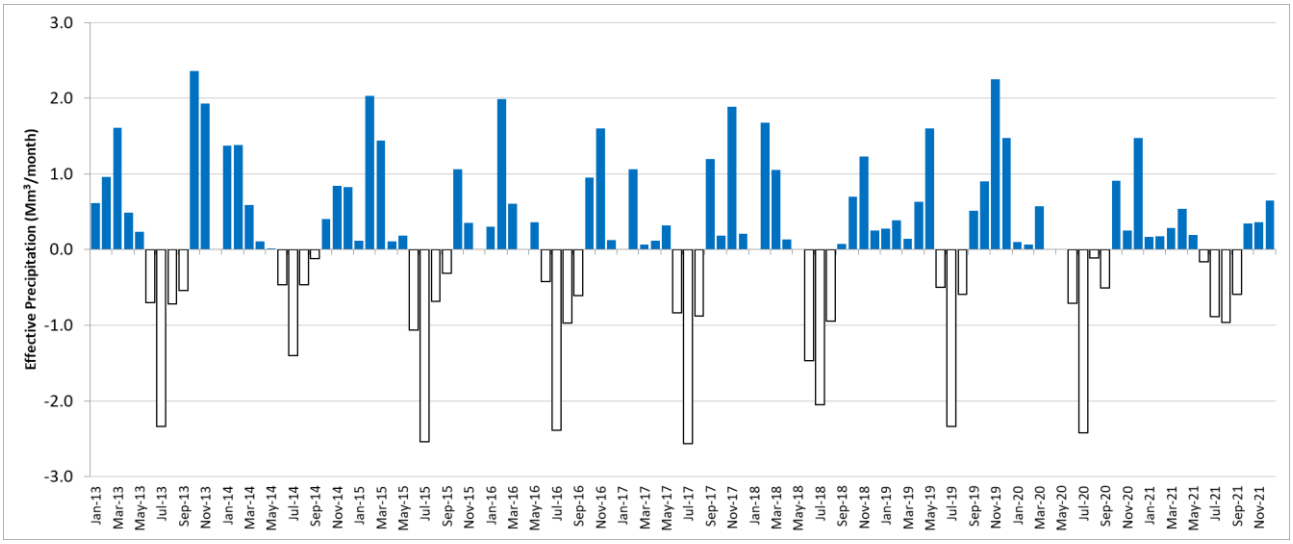

Figure 3-10. Effective precipitation assigned in the model as fluid flux boundary.

Table 3-1. Monthly effective rainfall rates assigned as fluid flux boundary in the model.

Date	Infiltration (mm/d)	Evapotranspiration (mm/d)	Effective Precipitation (mm/d)
Jan-13	1.3	0.0	1.3
Feb-13	2.2	0.0	2.2
Mar-13	3.3	0.0	3.3
Apr-13	1.0	0.0	1.0
May-13	0.5	0.0	0.5
Jun-13	0.0	-1.5	-1.5
Jul-13	0.0	-4.8	-4.8
Aug-13	0.6	-2.1	-1.5
Sep-13	0.2	-1.3	-1.1
Oct-13	4.9	-0.1	4.8
Nov-13	4.1	0.0	4.1
Dec-13	0.0	0.0	0.0
Jan-14	2.8	0.0	2.8
Feb-14	3.1	0.0	3.1
Mar-14	1.2	0.0	1.2
Apr-14	0.2	0.0	0.2
May-14	0.0	0.0	0.0
Jun-14	0.0	-1.0	-1.0
Jul-14	2.0	-4.8	-2.9
Aug-14	1.3	-2.2	-0.9
Sep-14	0.9	-1.2	-0.2
Oct-14	0.9	-0.1	0.8
Nov-14	1.8	0.0	1.8
Dec-14	1.7	0.0	1.7
Jan-15	0.2	0.0	0.2
Feb-15	4.6	0.0	4.6
Mar-15	3.0	0.0	3.0
Apr-15	0.2	0.0	0.2
May-15	0.4	0.0	0.4
Jun-15	0.0	-2.2	-2.2
Jul-15	0.0	-5.2	-5.2
Aug-15	0.5	-1.9	-1.4
Sep-15	0.5	-1.2	-0.7
Oct-15	2.2	0.0	2.2
Nov-15	0.7	0.0	0.7
Dec-15	0.0	0.0	0.0
Jan-16	0.6	0.0	0.6
Feb-16	4.3	0.0	4.3
Mar-16	1.2	0.0	1.2
Apr-16	0.0	0.0	0.0
May-16	0.7	0.0	0.7
Jun-16	0.0	-0.9	-0.9
Jul-16	0.0	-4.9	-4.9
Aug-16	0.4	-2.4	-2.0
Sep-16	0.1	-1.3	-1.3
Oct-16	2.0	-0.1	2.0
Nov-16	3.4	0.0	3.4
Dec-16	0.3	0.0	0.3
Jan-17	0.0	0.0	0.0
Feb-17	2.4	0.0	2.4
Mar-17	0.1	0.0	0.1
Apr-17	0.3	0.0	0.3
May-17	0.6	0.0	0.6
Jun-17	0.0	-1.8	-1.8
Jul-17	0.0	-5.2	-5.2
Aug-17	0.4	-2.2	-1.8
Sep-17	3.7	-1.2	2.5
Oct-17	0.4	-0.1	0.4
Nov-17	4.0	0.0	4.0
Dec-17	0.4	0.0	0.4
Jan-18	0.0	0.0	0.0
Feb-18	3.8	0.0	3.8
Mar-18	2.2	0.0	2.2
Apr-18	0.3	0.0	0.3
May-18	0.0	0.0	0.0
Jun-18	0.0	-3.1	-3.1
Jul-18	0.0	-4.2	-4.2
Aug-18	0.1	-2.0	-1.9
Sep-18	1.5	-1.4	0.2
Oct-18	1.5	-0.1	1.4
Nov-18	2.6	0.0	2.6
Dec-18	0.5	0.0	0.5
Jan-19	0.6	0.0	0.6
Feb-19	0.9	0.0	0.9
Mar-19	0.3	0.0	0.3
Apr-19	1.3	0.0	1.3
May-19	3.3	0.0	3.3
Jun-19	0.0	-1.0	-1.0
Jul-19	0.0	-4.8	-4.8
Aug-19	0.7	-2.0	-1.2
Sep-19	2.4	-1.3	1.1
Oct-19	1.9	-0.1	1.8
Nov-19	4.8	0.0	4.8
Dec-19	3.0	0.0	3.0
Jan-20	0.2	0.0	0.2
Feb-20	0.1	0.0	0.1
Mar-20	1.2	0.0	1.2
Apr-20	0.0	0.0	0.0
May-20	0.0	0.0	0.0
Jun-20	0.0	-1.5	-1.5
Jul-20	0.0	-5.0	-5.0
Aug-20	1.9	-2.1	-0.2
Sep-20	0.1	-1.2	-1.1
Oct-20	1.9	0.0	1.9
Nov-20	0.5	0.0	0.5
Dec-20	3.0	0.0	3.0
Jan-21	0.3	0.0	0.3
Feb-21	0.4	0.0	0.4
Mar-21	0.6	0.0	0.6
Apr-21	1.1	0.0	1.1
May-21	0.4	0.0	0.4
Jun-21	0.0	-0.3	-0.3
Jul-21	0.0	-1.8	-1.8
Aug-21	0.0	-2.0	-2.0
Sep-21	0.0	-1.3	-1.3
Oct-21	0.8	-0.1	0.7
Nov-21	0.8	0.0	0.8
Dec-21	1.3	0.0	1.3

3.4 Hydraulic and Transport Parameters

The model parameters pertaining to the variable-density flow and transport model are summarized in Table 3-2 and Table 3-3. The permeability is assumed to be homogeneous and isotropic in the horizontal directions, and anisotropic in the vertical for all model layers.

Table 3-2. Properties of groundwater used in the model.

Water compressibility	4.47E-10 $(kg/m.s^2)^{-1}$
Molecular diffusion coefficient	1E-9 m^2/s
Base concentration	0 g/L
Density of water at base concentration	998.9 g/L
Coefficient of density change with concentration	700 $(g\ water)^2$ / $(g\ solute.m^3\ water)$
Dynamic viscosity of water	1.1081×10^{-3} kg/(m.s)
Average temperature	16 °C

Table 3-3. Model parameters related to the coupled flow and transport models.

	Shallow silty sand aquifer (L1-L2)	**silty clay aquitard (L3-L5)**	**deep sand aquifer (L6-L7)**
Horizontal permeability	1.2E-10 m^2	1.0E-12 m^2	5.0E-12 m^2
Vertical anisotropy ratio for permeability	5		
Effective porosity	0.15	0.25	0.25
Longitudinal dispersivity	10 m		
Vertical anisotropy ratio for longitudinal dispersivity	100		
Transverse dispersivity	10 m		
Vertical anisotropy ratio for transverse dispersivity	10		

All EC measurement data are converted to total dissolved solids (i.e. solute) concentrations using a linear relationship developed in a hydrogeochemical characterization study of the Comacchio aquifer (Mastrocicco et al., 2012).

$$c = 0.873 \cdot EC \qquad \text{(Equation 4)}$$

Where EC is the electrical conductivity of the water sample in mS/cm, and c is the solute concentration of the water in g/L.

3.5 Calibration Data

A small data set of groundwater level measurements from one piezometer that has been recently installed in the town of Gorino is obtained for the modeling study. The time span of available measurements that are within the simulation time frame is from November 2020 until the end of 2021. The groundwater level and

salinity data of 14 months from this observation well are used for model calibration. Additionally, to compensate for the lack of calibration data auxiliary data is added to the calibration data set. It was amended with hypothetical head data from 20 virtual observation points, which are placed across the model domain. The observed groundwater levels at all virtual observation points are set slightly below the land surface to maintain a simulated water table height that does not exceed the land surface. The virtual observation points are placed such that they are present uniformly over the model area and between the ditches, where inundation of the land is possible. The location of the Gorino piezometer and the distribution of virtual observation points are shown in Figure 3-11.

Figure 3-11. Location of the Gorino piezometer and virtual observation points used in the model calibration.

3.6 Numerical Solver Settings

The conjugate gradient (CG) solver (Hestenes and Stiefel, 1952) is used for P solutions, and the ORTHOMIN solver (Vinsome, 1976) is used for C solutions. Various settings for the numerical solver methods are summarized in Table 3-4.

Table 3-4. Selected settings of the CG and ORTHOMIN solvers.

P solution solver	IC-preconditioned conjugate gradient
Max number solver iterations during P solution (ITRMXP)	300
Convergence tolerance for P solution	1E-09
Transport solution solver	ILU-preconditioned ORTHOMIN
Max number solver iterations during C solution (ITRMXU)	1000
Convergence tolerance for C solution	1E-09

4. MODEL CALIBRATION

This section of the deliverable describes calibration procedures, presents optimal parameter estimates, and a comparison of calibration targets to model-calculated hydraulic head values.

4.1 Calibration Procedure

Calibration is the process in which the model parameters are adjusted to improve the accuracy of the model and to demonstrate that the model is reasonably representative of observed site conditions. Calibration of the flow and transport model is accomplished by systematically perturbating model parameters and matching groundwater levels and salinity measured at the Gorino piezometer between November 2020 and December 2021 with the simulated pressures and concentrations. Simulated pressures and observed heads are converted to equivalent freshwater heads to ensure comparability.

Model calibration was performed in two phases; in the first phase, the model was calibrated manually (also called the trial-and-error method), which is the process of systematically changing model parameters, running the model with the changed input, and then comparing the result of the calibration with the calibration targets. The process was repeated until the simulated values compare favorably with the observed values. To evaluate calibration results and model accuracy quantitatively, the mean error (ME), mean absolute error (MAE), the sum of squared errors (SSQE), and root mean squared error (RMSE) are calculated for the observed head/concentration and modelled head/concentration data pairs for all 21 calibration targets.

The RMSE was calculated as:

$$RMSE = \sqrt{\frac{1}{n}\sum_{i=1}^{n}(h_m - h_s)_i^2} \qquad \text{(Equation 5)}$$

where

n is the number of residuals
h_m is the observed groundwater level at observation well i
h_s is the simulated hydraulic head at observation well i

The overall model accuracy is increased by minimizing the RMSE and the SSQE. However, the goal of the manual calibration was first to obtain a reasonable model solution that can be used as a starting point for automated calibration. Therefore, the goal was first to minimize ME values for each calibration target as much as possible, which implies matching the averages of observed and simulated values. In the second calibration phase, the manually pre-calibrated model was subject to automated parameter estimation, which resembles manual calibration except that a computer code rather than the user adjusts the model parameters. Here the goal was to minimize a composite objective function that is based on a combination of model errors (residuals).

The flow model was calibrated using the PEST parameter estimation computer code (Doherty, 2016). The automatic model calibration with PEST completes a single model simulation using a user-defined set of input

parameters and compares model outputs to the calibration dataset. Subsequent model runs were performed with small changes in model parameters, and the model outputs were compared again with the calibration dataset. The PEST code mathematically determines which input parameters to adjust to facilitate effective model calibration. It continued the process until an optimal set of model parameters was obtained, which provides the statistically best fit between model outputs and the calibration dataset. The PEST code implemented the Gauss-Levenberg-Marquardt algorithm. This algorithm is a gradient-based search method that adjusts parameters by attempting to minimize the sum of the squared and weighted residuals.

The calibration of the transient model is performed by matching modelled with measured hydraulic head and salinity concentrations recorded at the Gorino piezometer. The elevation of the piezometer measurement point is assumed as $z_{piezometer}$ = -2.42 m below sea level.

4.2 Calibration Parameters

Calibration parameters are defined to represent uncertain hydraulic properties of the model. Parameters adjusted during model calibration are horizontal permeabilities of each model layer, the vertical anisotropy ratio for permeability, the longitudinal dispersivity, and the effective porosities for each model layer. A total of 7 calibration parameters in 3 parameter groups were defined in the PEST calibration setup (Table 4-1). Initially assigned model parameters are used as prior information for the parameter estimation process to constrain the solution space. Ranges of plausible parameter values were identified for all calibration parameters (Table 4-1), which were implemented as lower and upper parameter limits in PEST.

Table 4-1. Calibration parameters, parameter value intervals, and calibrated parameter values.

Parameter Name	Parameter Description	Parameter Group	Lower Bound	Upper Bound	Calibrated Value	Units
Perm1	Permeability of silty-sand layer (L1-L2)	PERMs	1.20E-11	1.40E-09	1.4E-09	m^2
Perm2	Permeability of silty-clay layer (L3-L5))	PERMs	2.00E-13	5.00E-12	9E-13	m^2
Perm3	Permeability of lower sand layer (L6-L7)	PERMs	5.00E-13	5.00E-11	5E-11	m^2
Por1	Effective porosity of silty-sand layer (L1)	PORs	0.15	0.38	0.38	-
Por2	Effective porosity of silty-clay layer (L2)	PORs	0.15	0.50	0.45	-
Por3	Effective porosity of lower sand layer (L3)	PORs	0.15	0.35	0.2	-
D_L	Longitudinal dispersivity coefficient	DISPs	2.0	30.0	10	m
VANI_Perm	Vertical anisotropy ratio for permeability	PERMs	1.0	20.0	3.919	-

4.3 Calibration and Parameter Estimation Results

Calibration results are presented here as a report of model parameter estimates, and comparisons of calibration targets to model-calculated hydraulic head values and solute concentrations.

The 34 hydraulic head calibration targets for observation points in the Goro-Gorino model domain are compared with model-calculated hydraulic heads and concentrations at the same location and time as the observations. The head values were compared in terms of equivalent freshwater head. Pore pressure values as the primary output variable of the SUTRA model are converted to equivalent freshwater heads. Similarly, 14 solute concentration targets are compared with model-calculated concentrations. Using all calibration targets from 21 observation points, the RMSE values are 0.702 m and 3.282E-03 kg/kg for equivalent freshwater head and solute concentration, respectively. The mean values of absolute errors (MAE) were -0.659 m and 1.42E-03 kg/kg for head and concentration, respectively. The average model errors for each observation point are determined by calculating the average of all errors in time for a particular observation point. Model errors are calculated as observed minus simulated.

Observed values were plotted against simulated values and compared to a 1:1 perfect-fit line as shown in Figure 4-1 and Figure 4-2. The scatter of data points for heads is spread slightly below the 1:1 line, suggesting that simulated heads to a small degree are over-estimated. The simulated salinity concentrations display a relatively better fit. As expected, the PEST parameter estimation process improved model performance of the manually calibrated model.

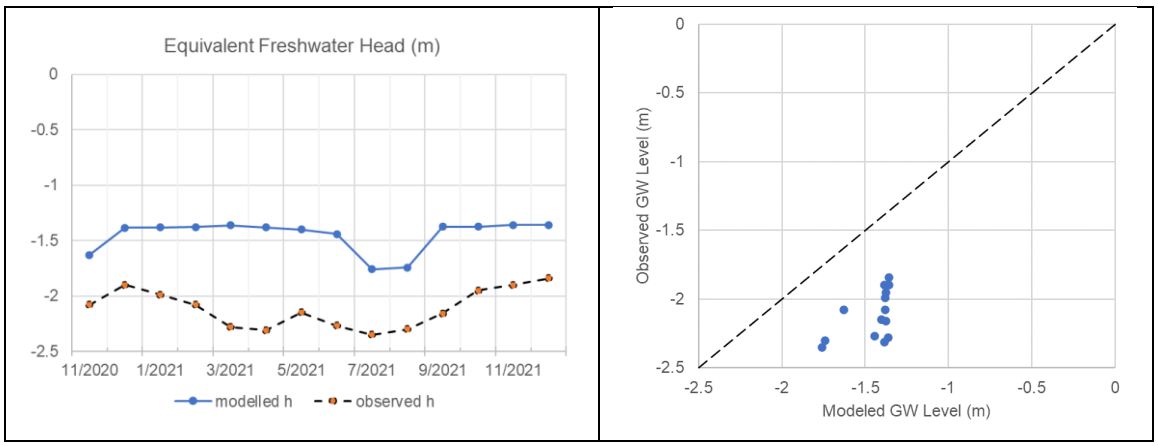

Figure 4-1. Comparison of observed and modelled equivalent freshwater heads (r^2=0.268) for calibration targets showing a 1:1 perfect-fit line for reference.

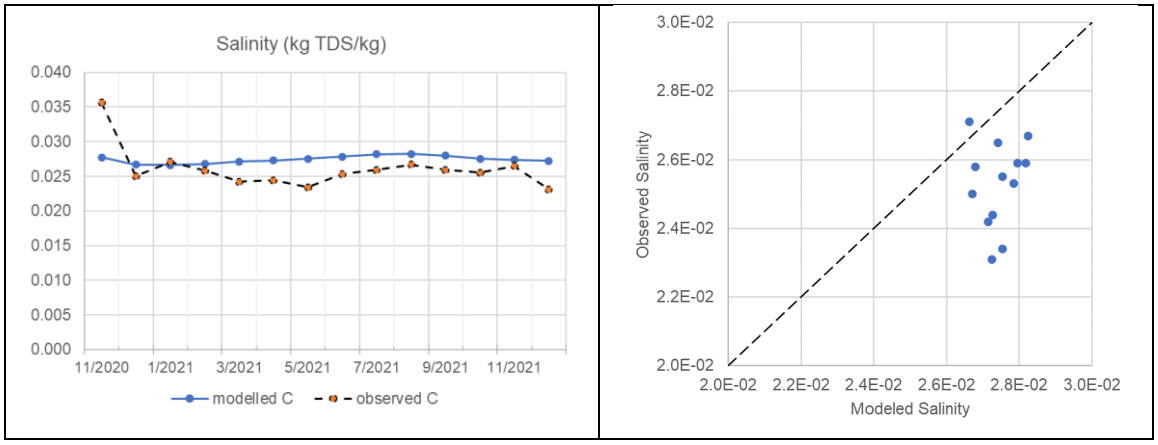

Figure 4-2. Comparison of observed and modelled salinity concentration for calibration targets showing a 1:1 perfect-fit line for reference.

5. MODEL RESULTS

In this section, the outcomes of the groundwater flow and solute transport simulation with the calibrated model for the Goro-Gorino site are presented. Results were analyzed in three parts; the analysis of groundwater flow and pore pressure distribution is provided in the first part; in the second part modeling results pertaining to seawater intrusion and solute transport are presented; the third part presents the modeling results related to the balances of water and solute masses. Although it is possible to post-process model results in many ways, the analysis of model results in this deliverable is limited to the mapping of simulated pore pressures and solute concentration distributions, plotting hydrographs, and processing of flow balance model outputs.

5.1 Simulated Groundwater Levels in the Goro-Gorino Aquifer

Simulated equivalent freshwater head hydrographs that are converted from modelled pore pressure are presented in Figure 5-1. Here it was evident that groundwater levels fluctuated between fixed intervals. Furthermore, a vertical hydraulic gradient can be identified causing a predominantly upward groundwater flow. More importantly, Figure 5-2 shows that the head in the uppermost layer is below the land surface throughout the simulation period.

The profile of the water table for a cross-section in the north-south direction is shown in Figure 5-3. Here the simulation of groundwater drainage in the shallow aquifer is visible, and it is demonstrated that the model has the ability to capture the drainage of groundwater to the reclamation ditches. It is confirmed that similar flow patterns are evident in other cross-section of the model domain.

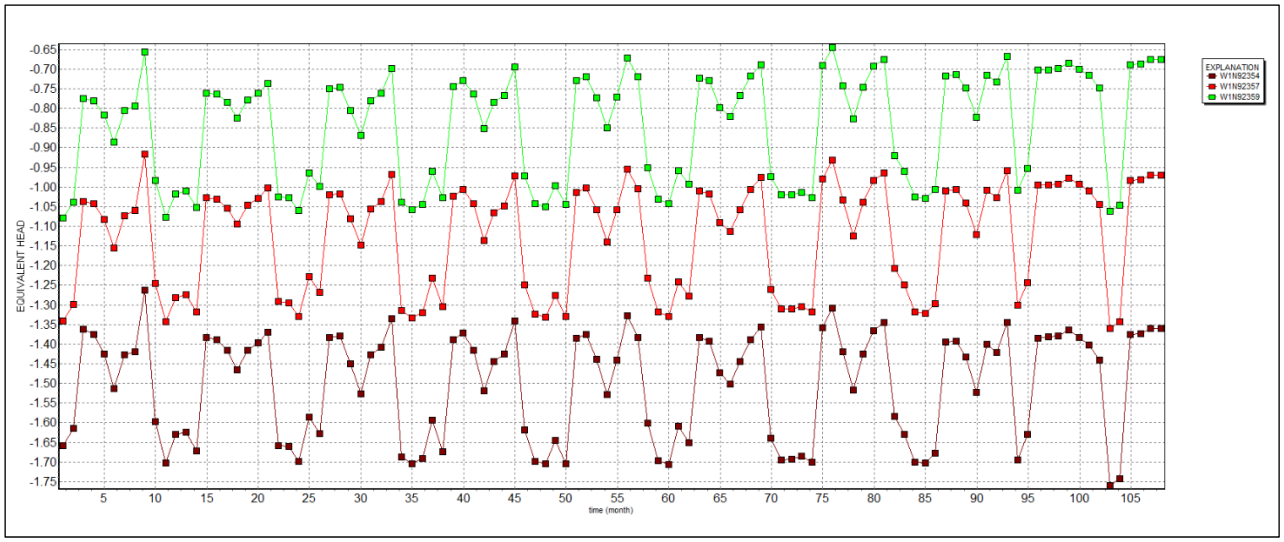

Figure 5-1. Simulated equivalent freshwater head (m) from Jan 2013 to Dec 2021 (9 years) at the Gorino piezometer showing hydrographs for the shallow aquifer (dark), silty clay aquitard (red), and deep sand layer (green).

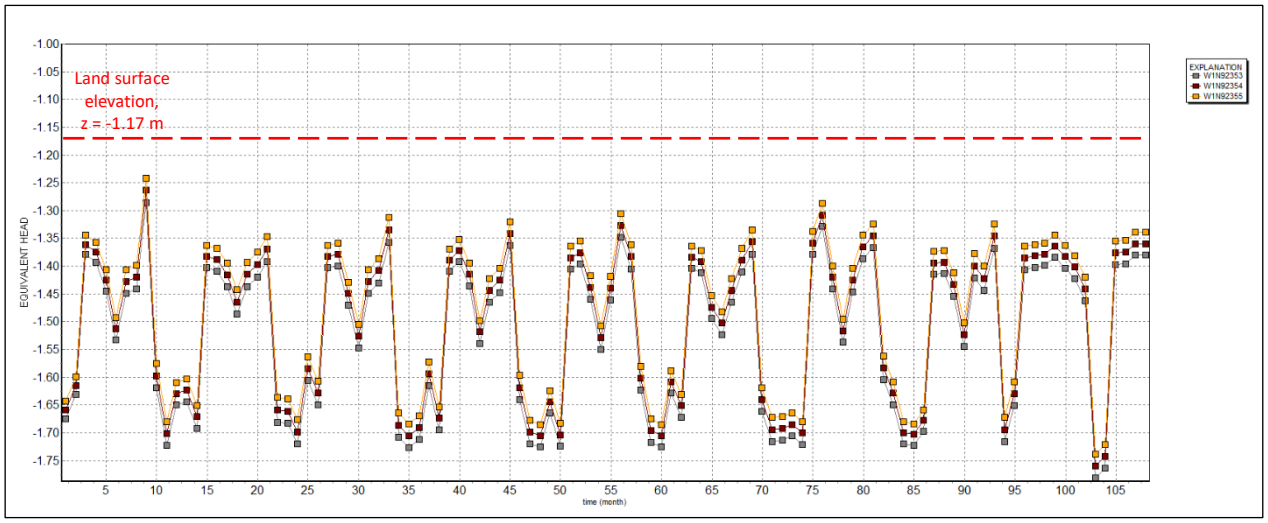

Figure 5-2. Simulated equivalent freshwater head (m) from Jan 2013 to Dec 2021 (9 years) at the Gorino piezometer showing hydrographs for different depths of the shallow aquifer.

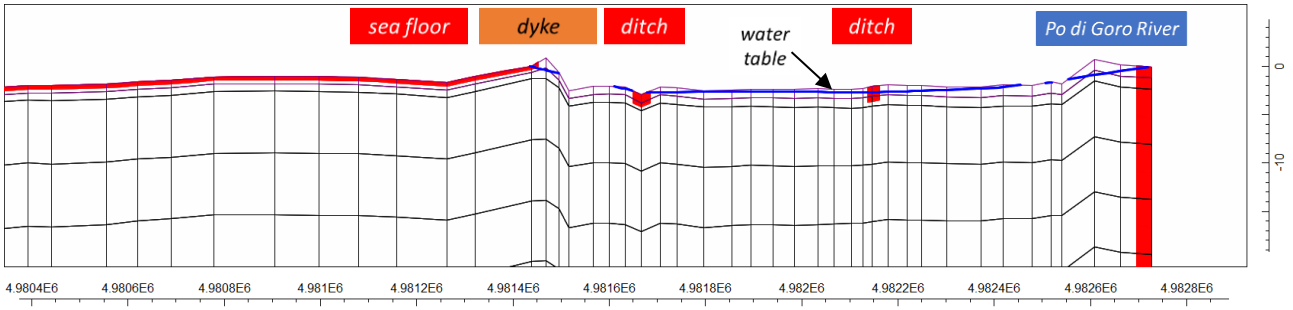

Figure 5-3. Simulated water table profile along a south-north cross-section of the model domain.

5.2 Simulated Salinity Concentrations in the Goro-Gorino Aquifer

The simulated solute concentration distribution at the end of the simulation period is shown in Figure 5-4. This distribution represents the salinity of the shallow silty sand aquifer. Based on this result it appears that brackish to brackish groundwater is present almost everywhere in the aquifer. Saline water ingresses from the sea and also from below the river. The area near Canale Bianco is largely unaffected. The relatively fresher water in the ditches is not sufficient to create any significant dilution in the groundwater. Furthermore, in some parts it can be observed that the intrusion of saline water is limited by some of the ditches. This implies that depending on the location, the ditches function as hydraulic barriers.

The temporal evolution of salinity in different stratigraphic units is provided in Figure 5-5. The solute concentration in the shallow aquifer fluctuates around a mean concentration of 27.4 g/l, with a minimum and maximum concentration of 21.2 and 29.8 g/l, respectively. The salinity in the silty clay layer is clearly higher with a mean concentration of 30.9 g/l. The groundwater in the deep sand layer has a concentration of 33.7 g/l, which almost equals that of seawater.

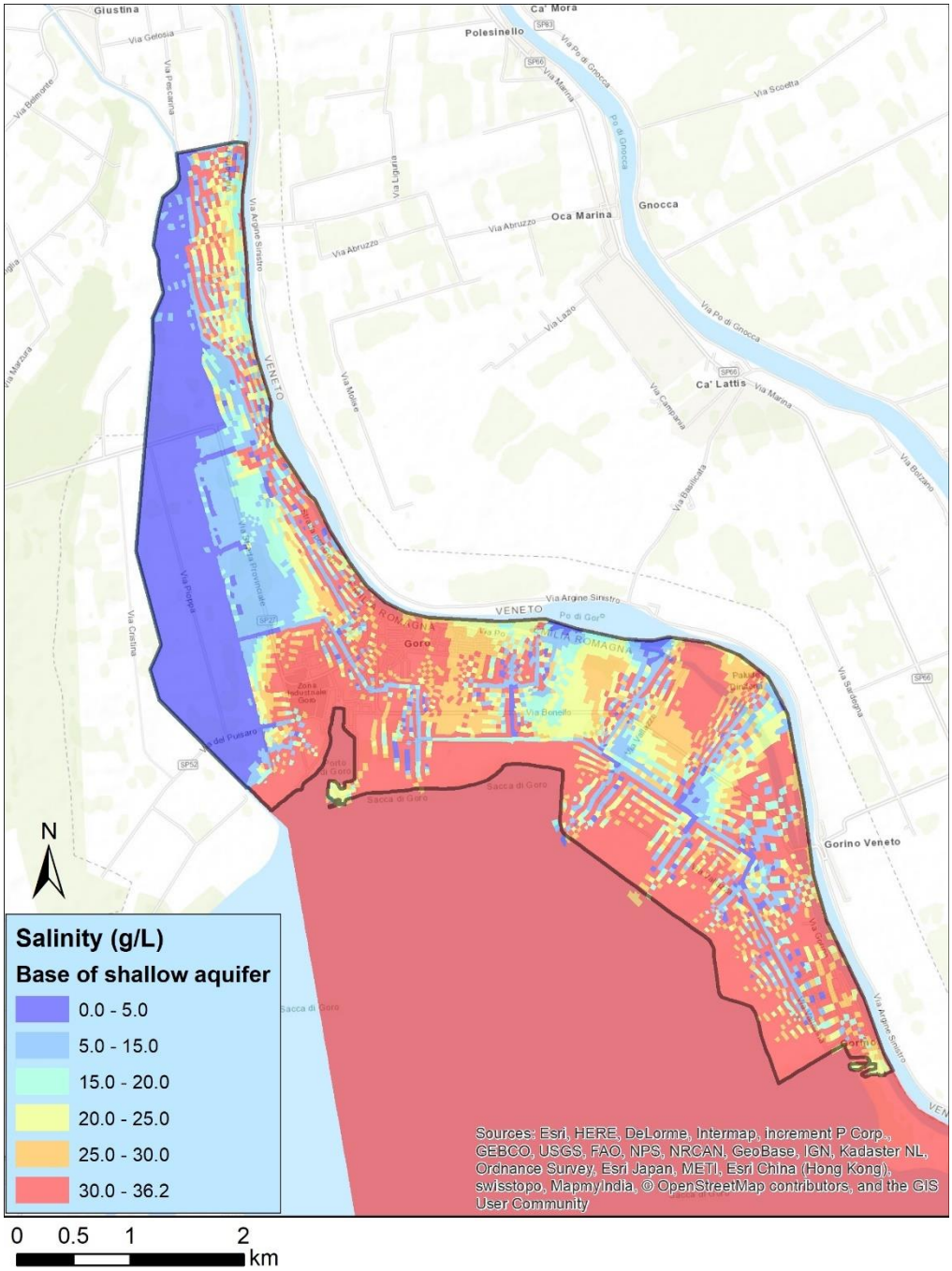

Figure 5-4. Simulated groundwater salinity concentration distribution after 108 model time steps (Dec 2021).

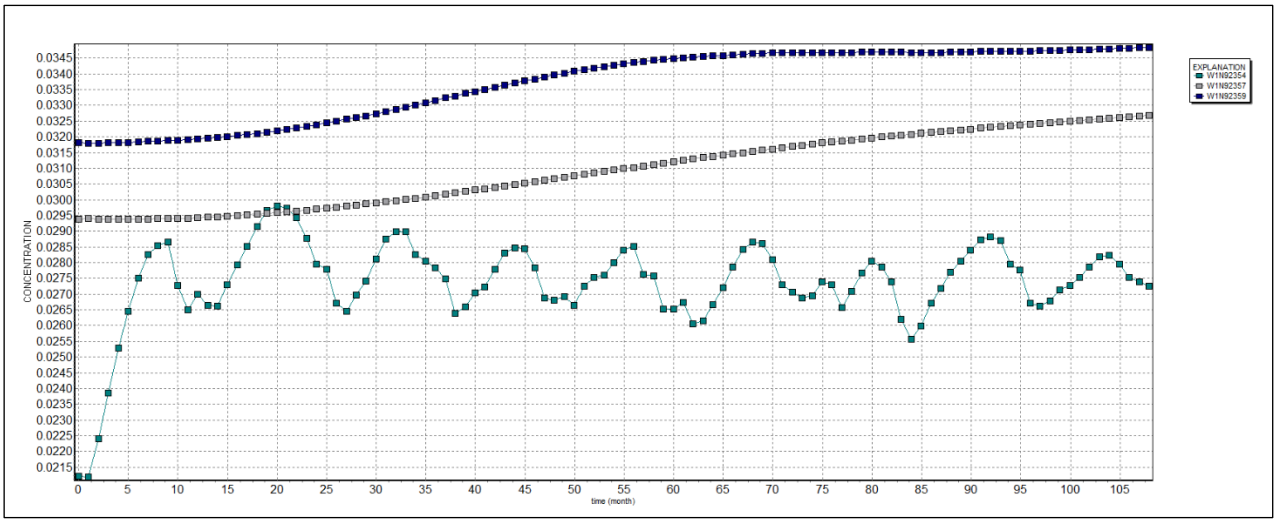

Figure 5-5. Simulated salinity concentration (kg TDS/kg) from Jan 2013 to Dec 2021 (9 years) at the Gorino piezometer showing results for the shallow aquifer (lower curve), silty clay aquitard (middle curve), and deep sand layer (upper curve).

To validate the model with an independent set of measurements, concentration profile measurements taken in July, August, and November in the year 2021 at the Gorino piezometers is used for comparison. The variability in the concentrations could not be captured with the model. However, the concentration increase with depth is confirmed by the data.

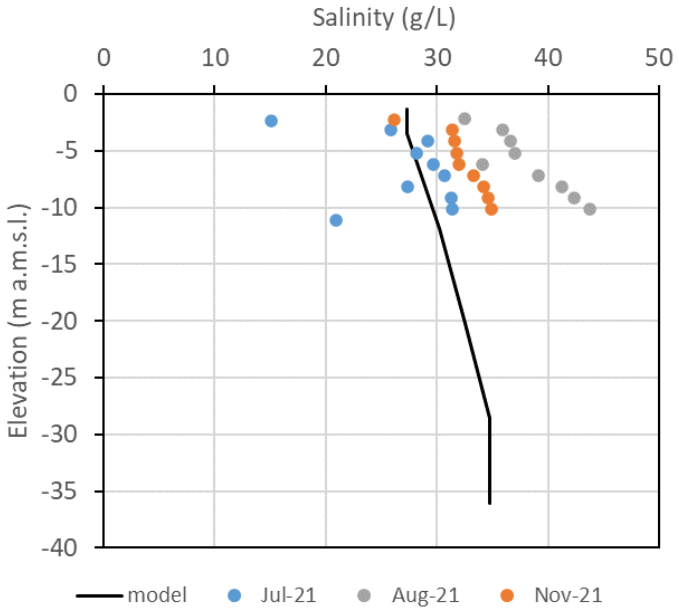

Figure 5-6. Profiles at the Gorino piezometer of modelled versus observed salinity concentrations.

5.3 Simulated Water and Solute Mass Balance

The simulated groundwater and solute mass balances quantify inflows and outflows to the Goro-Gorino aquifer. Mean annual mass fluxes are calculated using the model outputs and are presented in Figure 5-7 and Figure 5-8 in terms of influx, outflux and the difference. Most of the water enters the system from the saline delta layer below the Po di Goro, followed by the ditches and the river water itself. The main outflow components are the ditches and the river. In terms of net flux, the delta is the main source of water and the river appears to be the main sink.

From the resulting solute mass balance it can be concluded that among the solute influx components the delta layer has the highest proportion. According to the model results, the drainage system is the main sink of solutes, which removes annually an average of 30.978 million tons.

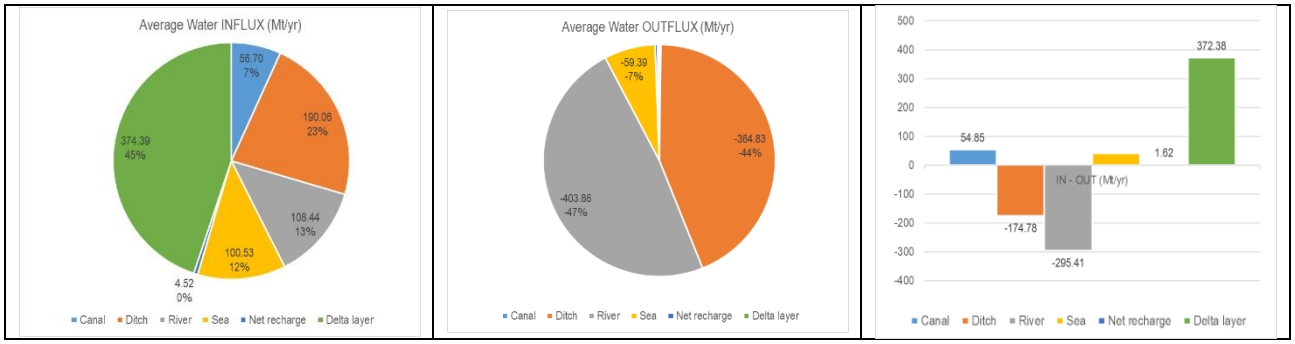

Figure 5-7. Simulated annual average water mass fluxes per boundary type.

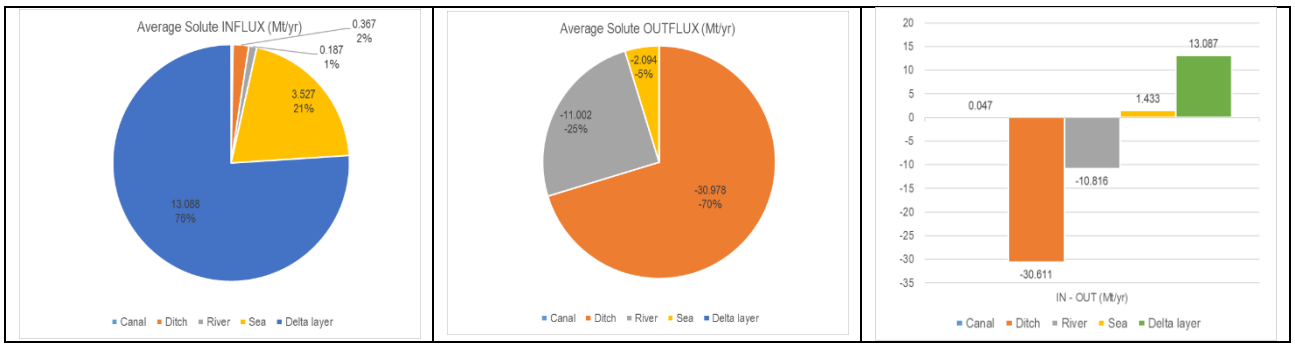

Figure 5-8. Simulated annual average solute mass fluxes per boundary type.

6. SUMMARY AND CONCLUSIONS

This report presents the results of a variable-density flow modeling study conducted for the Goro-Gorino site, which is part of the Comacchio aquifer. The model provides quantitative information about the status of salinization in the aquifer. Furthermore, it supports the process of understanding the mechanisms of salinization, the main sources and sinks for groundwater and solute mass fluxes. The mechanisms of salinization and the interplay of various sources and sinks can be further explored with the model, aiming at developing solutions to mitigate the salinization problem in the area.

The model presented here within the scope of the RESERVOIR project should be used with uncertainties in mind. There are also some limitations that should be noted while acknowledging that the conceptualization of the Goro Gorino site might have over-simplified the system. As with other flow and transport models for other sites, the accuracy and reliability of modeling results depend mostly on the accuracy/uncertainty of the input data. Therefore, the modeling process should be viewed as an iterative process where an effort to improve the model should be made if new information about the study site and the aquifer system is available.

For a better interpretation of model results the following limitations of the flow model should be considered when in the future the model is used for scenario analyses or other studies:

1) The heterogeneity of the aquifer could not be fully captured by the model. Heterogeneity in terms of permeability and porosity can be very effective on the distribution and travel time of solutes.
2) The available observation data to calibrate the model is not sufficient to obtain a model that can accurately simulate past and present conditions. More calibration data is needed to improve the model.
3) The potential influence of sea-level fluctuations is ignored.

REFERENCES

- Bondesan, M., Gatti, M., & Russo, P. , 1997. Vertical movements of the ground in the eastern Po Plain obtained from IGM data up to 1990 [Movimenti verticali del suolo nella Pianura Padana orientale desumibili dai dati IGM fino a tutto il 1990].
- Colombani, N., Mastrocicco, M., and Giambastiani, B. M. S., 2015. Predicting Salinization Trends in a Lowland Coastal Aquifer: Comacchio (Italy). Water Resources Management, 29(2), 603–618.
- Colombani, N., Osti, A., Volta, G., Mastrocicco, M., 2016. Impact of Climate Change on Salinization of Coastal Water Resources. Water Resour. Manag. 30, 2483–2496.
- Corbau, C.; Munari, C.; Mistri, M.; Lovo, S.; Simeoni, U., 2016. Application of the Principles of ICZM for Restoring the Goro Lagoon. Coast. Manage. 44, 350–365.
- Doherty, J., 2016. PEST, Model-independent parameter estimation—User manual parts I and II (6th ed.), Brisbane, Australia, Watermark Numerical Computing.

- Galbiati, L., Bouraoui, F., Elorza, F. J., and Bidoglio, G., 2006. Modeling diffuse pollution loading into a Mediterranean lagoon: Development and application of an integrated surface–subsurface model tool. Ecological Modelling, 193(1), 4–18.
- Giambastiani, B. M. S., Colombani, N., Mastrocicco, M., and Fidelibus, M. D., 2013. Characterization of the lowland coastal aquifer of Comacchio (Ferrara, Italy): Hydrology, hydrochemistry and evolution of the system. Journal of Hydrology, 501, 35–44.
- Hargreaves, G. H. and Samani, Z. A., 1985. Reference Crop Evapotranspiration from Temperature. Applied Engineering in Agriculture, 1(2), 96–99.
- Hestenes, M.R. and Stiefel, E., 1952. Methods of Conjugate Gradients for Solving Linear Systems. Journal of Research of the National Bureau of Standards. 49 (6), 409.
- Kjaer, J., 2002. Modelling the Hydrology and Nitrogen Dynamics in a Coastal Agricultural Catchment in the Mediterranean. Joint Research Centre, Environmental Institute, Ispra, Italy, EUR 21071EN.
- Mannini, P., Genovesi, R., and Letterio, T., 2013. IRRINET: Large Scale DSS Application for On-farm Irrigation Scheduling. Procedia Environmental Sciences, 19, 823–829.
- Mastrocicco, M., Giambastiani, B. M. S., Severi, P., and Colombani, N., 2012. The Importance of Data Acquisition Techniques in Saltwater Intrusion Monitoring. Water Resources Management, 26(10), 2851–2866.
- Simeoni U., & Corbau C., 2009. A review of the Delta Po evolution (Italy) related to climatic changes and human impacts. Geomorphology 107, 64-71.
- Stefani, M., & Vincenzi, S., 2005. The interplay of eustasy, climate and human activity in the late Quaternary depositional evolution and sedimentary architecture of the Po Delta system. Marine Geology, 222, 19-48.
- Teatini, P., Ferronato, M., Gambolati, G., & Gonella, M., 2006. Groundwater pumping and land subsidence in the Emilia-Romagna coastland, Italy: Modeling the past occurrence and the future trend. Water Resources Research, 42(1).
- Vinsome, P. K. W., 1976. Orthomin, an Iterative Method for Solving Sparse Sets of Simultaneous Linear Equations. SPE Symposium on Numerical Simulation of Reservoir Performance, SPE-5729-MS.
- Voss, C. I., and Provost, A.M., 2002 (Version of September 22, 2010). SUTRA, a model for saturated-unsaturated variable-density ground-water flow with solute or energy transport, U.S. Geological Survey Water-Resources Investigations Report 02-4231, 291 p.
- Winston, R.B., 2022. ModelMuse version 5.1.1: U.S. Geological Survey Software Release, 15 November 2022, https://doi.org/10.5066/P90QQ94D.